Elucidating the functional role of MLIP, a novel muscle A-type lamin interacting protein

Seham Rabaa, BSc (Hons)., BSocSc.

Thesis submitted to the Faculty of Graduate and Postdoctoral Studies, in partial fulfillment of the requirements for the M.Sc. degree in Biochemistry

Department of Biochemistry, Microbiology and Immunology
Faculty of Medicine
University of Ottawa

ABSTRACT

A-type lamin mutations are associated with degenerative disorders causing dilated cardiomyopathy, Charcot-Marie-Tooth neuropathy and Limb-Girdle Muscular Dystrophy. Our lab has identified MLIP; a novel protein that interacts with lamin A/C. Knocked down MLIP expression in C2C12 myoblasts down regulates myogenic regulatory factors, MyoD and Myogenin, which delays myogenic differentiation. We hypothesize that MLIP is essential for myogenic differentiation. Our goal is to define the MLIP associated pathways involved in myogenic programming. Gene expression profiling of MLIP stably knocked down C2C12 cells, identified 30 genes implicated in human disease. Mutations in five of those genes (*DMPK*, *HSPB8*, *LMNB2, NEFL* and *SGCD*) cause muscular dystrophy, neuropathies, and lipodystrophies that have phenotypic overlap with laminopathies. Further studies involving the MLIP knocked down cell lines demonstrated that in the absence of puromycin, MLIP protein expression returns to normal. This in turn affects the interpretation of the gene expression data and attempted MLIP recovery experiments.

ACKNOWLEDGEMENTS

I would like to thank my Supervisor for his guidance, mentorship, and the life lessons he has so kindly bestowed upon my fellow lab mates and me. To my past and present lab mates: thank you for patience and understanding in all matters that are science related. To my family: thank you for waking me up in the mornings, feeding me at night, and for loving me unconditionally.

Lastly, I leave you with one of my favourite quotes that have inspired me my whole life and will continue to inspire me:

"Seek knowledge from cradle to grave." Prophet Mohamad (PBUH)

TABLE OF CONTENTS

LIST OF ABBREVIATIONS

ABO	ABO blood group
Adarb1	Adenosind deaminase RNA-specific, B1
Aim1	Absent in melanoma 1
Ano5	Anoctamin 5
ANOVA	Analysis of variance
BCL2	B-cell CLL/lymphoma 2
Bmpr1b	Bone Morphogenetic prtein receptor, type IB
Capn10	Calpain 10
Ccr5	Chemokine (C-C motif) receptor 5
cDNA	complementary DNA
ChIP	Chromatin Immunoprecipitation
CMT2B	Charcot-marie-tooth neuropathy type 2B
CO2	carbon dioxide
DAPI	diamidino-2-phenylindole
DAVID	Database for Annotation, Visualization and Integrated Discovery
DCM	Dilated cardiomyopathy
DCM1A	Dilated cardiomyopathy type 1A
DH5α	*Escherichia coli* strain
DM	Differentiation Medium
DMD	Duchenne muscular dystrophy
DMEM	Dulbecco's modified Eagle's medium
Dmpk	Dystrophia Myotonica-protein kinase
DTT	Dithiothreitol
EDMD	Emery-Dreifuss Muscular Dystrophy
EDTA	Ethylenediaminetetraacetic acid
EYA1	Eyes absent homolog 1
FBS	fetal bovine serum
FPLD	Dunnigan type familial partial dystrophy
GAPDH	Glyceraldehye-3-phosphate dehydrogenase
GFP	Green fluorescent protein
GM	growth medium
Hcrt	Hypocretin (orexin) neuropeptide precursor
HGPS	Hutchinson-gilford progeria syndrome
Hmga2	High mobility group AT-hook 2
HRP	horseradish peroxidase
HS	horse serum
HSPB8	Heat shock 22kDa protein 8
IF	Intermediate filaments
Ig	Immunoglobin
IgG	Immunoglobin G
INM	Inner nuclear membrane
IP	immunoprecipitation
JAK2	Janus Kinase 2
KD	Knockdown

kDa	KiloDalton
KO	Knockout
LB	Luria-Bertani
LGMD1B	Limb girdle muscular dystrophy type 1B
LMNA	Lamin A/C gene
LMNB1	Lamin B1 gene
LMNB2	Lamin B2 gene
MARVELD2	MARVEL domain containing 2
MEF2C	Myocyte enhancer factor 2 C
MHC	Myosin heavy chain
MLIP	Muscle A-type lamin Interacting Protein
MRF	Myogenic regulatory factors
MRF4	myogenic regulatory factors 4
MyBPC	myosin binding protein
MyoD	myoblast determination protein 1
NCBI	National Centre for Biotechnology Information
NE	Nuclear envelope
NEB	New England Biolabs
NEFL	Neurofilament, light peptide
NIH	National Institutes of Health
NLS	Nuclear localization signal
Oct4	Octamer binding transcription factor 4
OMIM	On-line Mendelian Inheritance in Man
ONM	Outer nuclear membrane
PBS	phosphate-buffered saline
PCR	polymerase chain reaction
PML	Promyelocytic leukemia
PMSF	Phenylmethylsulphonyl fluoride
pRB	Retinoblastoma protein
PVDF	Polyvinylidene Fluoride
QC	Quality control
RXRα	Retinoic acid receptor alpha
RMA	Robust Multichip Average
SDS	sodium dodecyl sulfate
SDS-PAGE	Sodium dodecyl sulfate Polyacrylamide gel electrophoresis
SGCD	Sarcoglycan, delta
SIX	Sine oculis homeobox
Sh2d1a	SH2 domain protein 1A
shRNA	Short hairpin RNA
shRNAmir	Short-hairpin mircroRNA
SFM	serum free media
TBST	Tris-Base Tween-20
tGFP	Turbo Green fluorescent protein
TF	Transcription factors
WT	Wild type
Y2H	Yeast-two-hybrid

LIST OF FIGURES

Supplementary Figures

LIST OF TABLES

Supplementary Tables

Chapter 1: Introduction

1.1 Nuclear Envelope

The eukaryotic cell has evolved to develop a multifaceted network of proteins that make up lipid bi-layers used to compartmentalize and protect organelles such as the nucleus. The nucleus consists of a double lipid bi-layer referred to as the nuclear envelope (NE), which protects the nuclear content from the rest of the cell. The NE is made up of the outer nuclear membrane (ONM) and the inner nuclear membrane (INM), both of which are lipid bi-layers (Gruenbaum *et al*, 2005). The NE is very dynamic where proteins are shuttled in and out of the nucleus through nuclear pore complexes (NPCs) (Figure 1) (Gruenbaum *et al*, 2005; Capell *et al*, 2006). Underlying the INM is a second structure called the nuclear lamina and it is involved in transcriptional regulation (Figure 1) (Gruenbaum *et al*, 2005; Capell *et al*, 2006).

1.1.1 The Nuclear Lamina

The nuclear lamina is a complex network of proteins, composed primarily of filamentous structures such as lamins A, B1, B2, and C and protein binding partners (Figure 1). This mesh of proteins also acts as a region for transcriptional activity and chromatin remodeling, while maintaining both shape and structural stability of the nucleus (Capell *et al*, 2006). Disruptions of the lamina, primarily of the lamins, can manifest as diseases, such as Emery-Dreifuss muscular dystrophy (EDMD). Lamins are type V intermediate filament proteins that interact as coiled-coil dimers in a head-to-tail fashion and are key proteins that maintain the nuclear lamina (Andres and Gonzalez, 2009).

Figure 1 Structure and function of the nuclear lamina. The nuclear lamina lies on the inner surface of the inner nuclear membrane (INM), where it serves to maintain nuclear stability, organize chromatin and bind nuclear pore complexes (NPCs) and a steadily growing list of nuclear envelope proteins (purple) and transcription factors (pink). Nuclear envelope proteins that are bound to the lamina include nesprin, emerin, lamina-associated proteins 1 and 2 (LAP1 and LAP2), the lamin B receptor (LBR) and MAN1. Transcription factors that bind to the lamina include the retinoblastoma transcriptional regulator (RB), germ cell-less (GCL), sterol response element binding protein (SREBP1), FOS and MOK2. Barrier to auto-integration factor (BAF) is a chromatin-associated protein that also binds to the nuclear lamina and several of the aforementioned nuclear envelope proteins. Heterochromatin protein 1 (HP1) binds both chromatin and the LBR. ONM, outer nuclear membrane. Reprinted by permission from Macmillan Publishers Ltd: Capell and Collins. Human laminopathies: nuclei gone genetically awry. *NatureReviews Genetics* 7, 940–952 (December 2006).

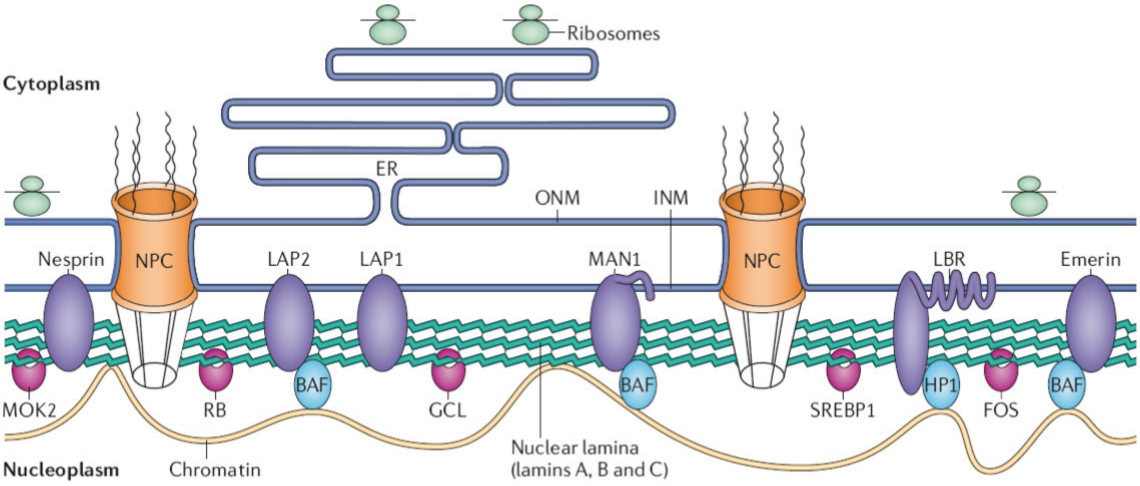
Ribosomes
Cytoplasm
ER
ONM
INM
Nesprin
NPC
LAP2
LAP1
MAN1
NPC
LBR
Emerin
MOK2
RB
BAF
GCL
BAF
SREBP1
HP1
FOS
BAF
Nucleoplasm
Chromatin
Nuclear lamina
(lamins A, B and C)

1.2 Lamins

There are two groups of lamins: the A-type lamins, which include lamins A, AΔ10, C, and C2, where lamins A and C are the major products; and the B-type lamins such as lamins B1, B2, and B3, where lamins B1 and B2 are the major products (Capell *et al*, 2006). A-type lamins are encoded by the *LMNA* gene (which is found on chromosome 1q21.2) and are products of alternative splicing (Lin and Worman, 1993; Wydner *et al*, 1996). The *LMNB1* gene, which is found on chromosome 5q23.2, encodes lamin B1 and the *LMNB2* gene, which is found on chromosome 19p13.3, encodes lamin B2 (Biamonti *et al*, 1992; Lin and Worman, 1995). Lamins contain a highly conserved α-helical central rod domain, a carboxy (C)-terminal tail domain and an amino (N)-terminal globular domain that varies in sequence amongst different lamin proteins (Figure 2) (Fisher *et al* 1986; McKeon *et al* 1986).

The α-helical central rod domain is involved in forming coiled-coil dimers, which then associate in an anti-parallel manner forming a protofilament (Heitlanger *et al*, 1992; Burke *et al*, 2001). Furthermore, the C-terminal domain contains a nuclear localization signal (NLS) and an immunoglobin (Ig)-like structure (Fisher *et al* 1986; McKeon *et al* 1986; Krimm *et al*, 2002).

Figure 2 *LMNA* gene mutations and associated diseases The LMNA gene (introns not to scale) is 57.6 kb long and consists of 12 exons, encoding two globular domains and a central α-helical coiled-coil rod domain. Lamin C (not shown) is encoded by exons 1 to 9 and a portion of exon 10. Lamin A results from alternative splicing, which adds exons 11 and 12 and removes the lamin-C-specific portion of exon 10. Examples of the main mutations that cause laminopathies are shown above the gene; not all mutations are listed. A more complete list can be obtained at the Leiden Muscular Dystrophy pages and OMIM. In the case of HGPS, MAD, FPLD, AR-EDMD, RD and CMT2B1, the most common causative LMNA mutation (or only mutation) is shown. In the cases of AD-EDMD, AWS, LGMD1B, GLD and DCM1A, a representative mutation among multiple causative mutations is included. AD-EDMD, autosomal dominant Emery–Dreifuss muscular dystrophy; AR-EDMD, autosomal recessive Emery–Dreifuss muscular dystrophy; AWS, atypical Werner syndrome; CMT2B1, Charcot–Marie–Tooth disorder, type 2B1; DCM1A, dilated cardiomyopathy, type 1A; FPLD, Dunnigan familial partial lipodystrophy; GLD, generalized lipodystrophy; HGPS, Hutchinson–Gilford progeria syndrome; LGMD1B, limb girdle muscular dystrophy, type 1B; MAD, mandibuloacral dysplasia; RD, restrictive dermopathy. Reprinted by permission from Macmillan Publishers Ltd: Capell and Collins. Human laminopathies: nuclei gone genetically awry. *NatureReviews Genetics* 7, 940–952 (December 2006).

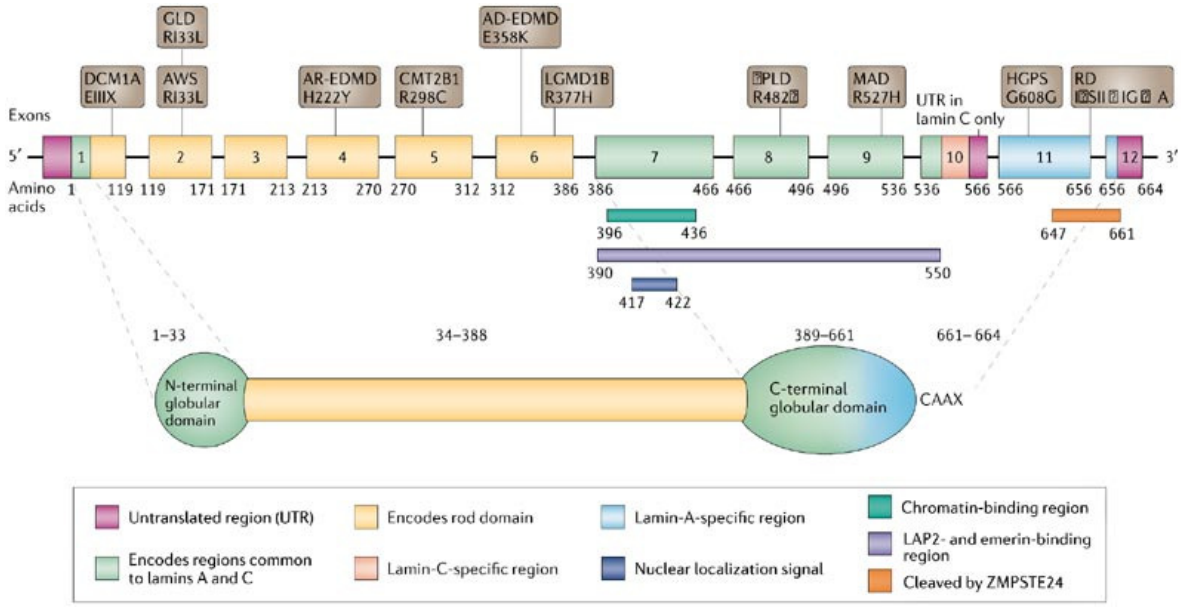

Lamins undergo post-translational modifications. For example, during mitosis lamins are phosphorylated causing the depolymerization of the lamina and separation of lamins from chromatin and the INM proteins (Gerace and Blobel, 1980; Nigg, 1992; Worman *et al*, 2009). All lamins except for lamins C and C2 contain a CAAX motif within the C-terminal tail (where C is cysteine, A is an aliphatic amino acid and X represents any amino acid), that signals for farnesylation, the addition of a 15-carbon farnesyl lipid (Zhang and Casey, 1996; Dauer and Worman, 2009). Then endoproteases (such as RCE1 and ZMPSTE24) cleave the -AAX motif and a carboxymethyl group is added by the ICMT membrane methyltransferase (Beck *et al*, 1990; Maske *et al*, 2003; Dauer and Worman, 2009). Prelamin A undergoes a final endoproteolytic cleavage by ZMPSTE24 to form mature lamin A (Beck *et al*, 1990; Maske *et al*, 2003; Dauer and Worman, 2009). Otherwise, in B-type lamins the processing is completed once the C-terminus is carboxymethylated (Beck *et al*, 1990; Maske *et al*, 2003; Dauer and Worman, 2009).

Both groups of lamins are structurally and functionally different; A-type lamins are expressed only in differentiated cells and are seen in a tissue specific manner (Rober *et al*, 1989; Gruenbaum *et al*, 2005) and B-type lamins are expressed during the course of development in all cells (D'Angelo and Hetzer, 2006; Vergnes *et al*, 2004). The different expression patterns exhibited by both groups of lamins imply that A-type lamins may be involved in attaining differentiation (Holaska, 2008).

1.3 Laminopathies

Laminopathies are defined as diseases resulting from mutations of the nuclear lamina; primarily those of the lamins and lamin associated proteins (Table 1). The majority

of laminopathies are a result of *LMNA* mutations (or A-type Laminopathies) where a minimum of 12 diseases can be traced back to it, conversely only a few diseases are due to B-type lamin gene mutations (Worman *et al*, 2010). There are over 400 mutations spread throughout *LMNA* (Merlini 2001; http://umd.be//LMNA/). Figure 2 depicts *LMNA* and identifies some of the mutations causing A-type laminopathies. Many *LMNA* mutations affect striated muscle and can cause Emery-Dreifuss muscular dystrophy (EDMD), limb-gridle muscular dystrophy type 1B (LGMD1B), and dilated cardiomyopathy1A (DCM1A) (Worman *et al*, 2009; Worman *et al*, 2010). EDMD can also be caused by mutations of the *EMD* gene; *EMD* encodes the emerin protein (Bione *et al*, 1994; Worman *et al* 2009). Emerin is a protein that binds to A-type lamins and is a vital part of the INM (Nagano *et al*, 1996). Muscular dystrophies cause muscle weakness and wasting, where most cases lead to cardiomyopathy (Worman *et al*, 2009; Worman *et al*, 2010). Mutations of *EMD* that cause EDMD also cause cardiomyopathy (Bione *et al*, 1994, Worman *et al* 2009).

Table 1. Diseases associated with mutations in lamins and other nuclear lamina proteins. Adapted from Worman *et al*, 2009; Capell and Collins, 2006.

Gene Name	Disease	Phenotype
Striated Muscle		
LMNA	Emery-Dreifuss Muscular Dystrophy (EDMD)	Muscle wasting and dilated cardiomyopathy
LMNA	Dilated Cardiomyopathy (DCM)1A	Weakened, enlarged heart, poor pumping of blood
LMNA	Limb Girdle Muscular Dystrophy (LGMD)1B	Muscle wasting, affecting upper and lower limbs and extremities, DCM.
EMD	EDMD	Muscle wasting, DCM
LAP2 (TMPO)	Dilated Cardiomyopathy (DCM)	Weakened, enlarged heart, poor pumping of blood
Lipodystrophy		
LMNA	Familial Partial Lipodystrophy-Dunnigan (FPLD) 2	Loss of fat in limbs but accumulation in neck and face, hypertrigliceridemia, diabetes
LMNA	Mandibuloacral dysplasia	Partial lipodystrophy, face deformities
LMNB2	Acquired Partial Lipodystrophy	Loss of fat in upper body and upper limbs but accumulation in lower body
Neuropathy		
LMNA	Charcot-Marie-Tooth Disorder (CMT) 2B1	Muscle weakness and loss of reflexes in lower limbs
LMNB1	Adult onset autosomal dominant leukodystrophy (ADLD)	Symmetrical loss of myelin throughout CNS
Progeria		
LMNA	HGPS	Aged appearance, alopecia, stunted growth, loss of fat, osteoporosis, cardiovascular disease
ZMPSTE24	Restrictive Dermopathy (RD)	Loss of fat, taught skin, perinatal lethal, alopecia, bone deformities
LMNA	Atypical Werner Syndrome	Aged appearance, cataracts, stunted growth, osteoporosis, cardiovascular disease
Other		
LBR	Pelger-Huet anomaly	Deformed neutrophils, short limbs, abnormal bone structure

Mutations causing Dunnigan-type familial partial lipodystrophy (FLPD) are found primarily within exon 8 of *LMNA*, which encodes for an Ig-like fold structure in lamins (Shackleton *et al*, 2000; Krimm *et al*, 2002). This is a disease that causes the loss of subcutaneous fat from the limbs and accumulation of fat within the face and neck, followed by the onset of diabetes mellitus (Worman and Bonne, 2009). *LMNA* mutations can manifest as neuropathies such as Charcot-Marie Tooth (CMT) type 2 peripheral neuropathy, where R298C mutation causes nerve degeneration and muscle wasting of the lower limbs (Capell and Collins, 2006; Worman *et al*, 2009).

One of the more serious *LMNA* associated diseases is progeria, a group of disorders that are defined by premature aging. One such example is Hutchinson-Gilford progeria syndrome (HGPS), which is characterized by alopecia, decreased subcutaneous fat, and early atherosclerosis. These symptoms lead to death due to a heart attack or a stroke, within the teenaged years of one's life (Andres and Gonzalez, 2009; Capell and Collins, 2006). Progeria is caused by an incompletion in processing premature lamin-A, where the final endoproteolytic cleavage by ZMPSTE24 does not occur (Reddel and Weiss, 2004; Goldman *et al*, 2004). In turn, this yields a protein called progerin that alters the nuclear lamina structure (Reddel and Weiss, 2004; Goldman *et al*, 2004). This forms a crenated nucleus and disrupts chromatin interactions (Reddel and Weiss, 2004; Goldman *et al*, 2004). One of the many mutations causing HGPS is *LMNA* mutation C1824T, which triggers a cryptic splice site preventing proper cleavage of prelamin A (Scaffidi P and Mistedli T, 2008). This is believed to lead to poor maintenance of mesenchymal stem cell populations and subsequent depletion of and defective differentiation of stem cell pools (Scaffidi P and Mistedli T,

2008). Moreover, mutations in *ZMPSTE24* also cause progeroid syndrome (Worman *et al*, 2010).

Until now, only two clinically identified diseases are due to B-type lamin mutations where *LMNB1* duplication causes adult-onset autosomal dominant leukodystrophy, leading to complete shutdown of the central nervous system (CNS). The second disorder is the result of point mutations within *LMNB2* that causes acquired partial lipodystrophy (Padiath *et al*, 2006; Hegele *et al*, 2006).

From the above given examples, it is clear that *LMNA* mutations and their associated disorders can be classified into two groups: tissue specific phenotypes and systemic (multi-system) disorders (Dauer and Worman, 2009; Capell and Collins, 2006). It is not clear why one would see tissue specific disorders when A-type lamins are expressed in most differentiated cells, although two major hypotheses have been proposed: the structural and the gene expression hypotheses. The structural hypothesis states that defects in the NE would weaken it and cause cell death under conditions of high mechanical stress (which potentially explains some myopathies) (Hutchison, 2002). Alternatively, the gene expression hypothesis asserts that mutated NE proteins interfere with transcription factor binding of chromatin, by preventing key interactions with regulatory proteins (Hutchison, 2002).

Although the majority of laminopathies are A-type specific and can cause muscular dystrophies, not all muscular dystrophies and neuropathies are lamin related. Regardless of the cause, muscular dystrophies still present the same or similar phenotypes. For example, there are over a dozen types of LGMD that are not due to *LMNA* mutations but are caused by mutations in other proteins such as the sarcoglycans family of proteins and fukutin

(Guglieri *et al*, 2008). Furthermore, CMT is due to mutations found in many genes other than *LMNA*, such as *NEFL*, *HSPB1* and *HSPB8* (Casasnovas *et al*, 2008).

Laminopathies such as EDMD and LGMD target striated muscle and thus understanding the involvement of lamin A/C in skeletal myoblast differentiation may help to identify effective treatments for these diseases.

1.4 Skeletal Myogenesis

Skeletal myogenesis is controlled by several groups of transcription factors, primarily the myogenic regulatory factors (MRFs). This includes MyoD, myogenin, Myf5, and Mrf4 (Myf6). These factors regulate differentiation of myoblasts, allowing them to fuse into myotubes (Parker *et al*, 2003). Satellite cells are muscle specific progenitor cells and are located along the myofibers (Kuang *et al*, 2008; Perdiguero *et al*, 2009). They differentiate to form myoblasts used to make the muscle fibers (Kuang *et al*, 2008; Perdiguero *et al*, 2009). Satellite cells are marked by the expression of Pax7, a paired-box (Pax) transcription factor. Upon muscle injury or regeneration, Pax7 activates the cells to a proliferative state, recruiting first Myf5 and then MyoD (Olguin and Olwin, 2004; Zammit *et al*, 2004). This stimulates the cell to become a myoblast, triggering cell cycle arrest and driving differentiation (Andres and Walsh, 1996; Parker *et al*, 2003; Olguin and Olwin, 2004; Zammit *et al*, 2004). MyoD is crucial for cell cycle arrest since it associates with hypophosphorylated pRB (retinoblastoma protein) leading to cell cycle withdrawal (Gu *et al*, 1993; Sabourin and Rudnicki, 2000). Myogenin and MRF4 mark late differentiation; they are required for myotube formation (Andres and Walsh, 1996; Sabourin and Rudnicki, 2000).

pRb also forms a complex with the E2F family of transcription factors which interact with lamin A/C and lamin-associated polypeptide 2α (LAP2α) (Johnson *et al*, 2004; Maraldi *et al*, 2010). Furthermore, *LMNA* mutations in C2C12 mouse myoblast cells disrupt pRB-LAP2α complexes (Markiewicz *et al*, 2005) and LMNA mutation R453W (which causes EDMD) can prevent myoblast differentiation (Favreau *et al*, 2004).

Therefore, understanding how muscle development is associated with diseases is crucial to future studies. Discovering new players that interact with lamins may be a starting point to finding potential therapeutics and treatments. The C2C12 mouse myoblast cell line is a well established immortalized cell line that has been used to study myogenesis, laminopathies, and muscular dystrophies since it expresses MRFs, lamins, and can be easily manipulated to differentiate into myotubes (Yaffe and Saxel, 1977; Blau *et al*, 1983; Chen *et al*, 2006, Maroldi *et al*, 2010). For these reasons, the C2C12 cell line is an ideal model cell line to study myogenesis.

1.5 Discovery of MLIP

Muscle A-type Lamin interacting Protein (MLIP) is a novel non-homologous, single copy gene found in all amniotes. It was discovered through a yeast two-hybrid screen where the first 230 amino acids (aa) of the Rod-1 domain of lamin A/C (LMNA) gene was used as the bait against a pooled human heart complementary DNA library (Matchmaker cDNA library, Clontech). Out of approximately 3.5 x 10^6 clones in the library, 232 positively identified clones were sequenced and of those, 6 independent clones were homologous to the Chromosome 6 open reading frame 142 (C6orf142, GenBank number NM_138569) in humans. In mice, MLIP is called 2310046A06Rik and is found on chromosome 9 E1. *In*

vitro pull-down assays using a recombinant hexa-histadine-MLIP and GST-Lamin-Rod 1 domain was performed to show that MLIP does indeed interact with the Rod 1 domain of LMNA.

The MLIP gene spans 247 kilobases (kb) with 13 exons that encodes for a protein 458 aa with no known structural or functional domains. The online database GEO Profiles (sponsored by NCBI) depicts gene expression and molecular abundance profiles, based on published microarray data. It reveals that 443 hits displays MLIP regulation under different conditions. Of the 443 hits, 68 are related to muscle development and regulation.

Figure 3: MLIP expression profile from mouse tissues and immortalized cell lines (**A)** Normalized tissue distribution of MLIP expression in adult mice (n=3) as determined by real-time PCR **B)** Western blot analysis of MLIP protein expression in mouse tissues and mouse derived cell lines, C2C12 myoblast, HL-1-heart derived cells, 10T1/2- mouse clonal embryo.

A.

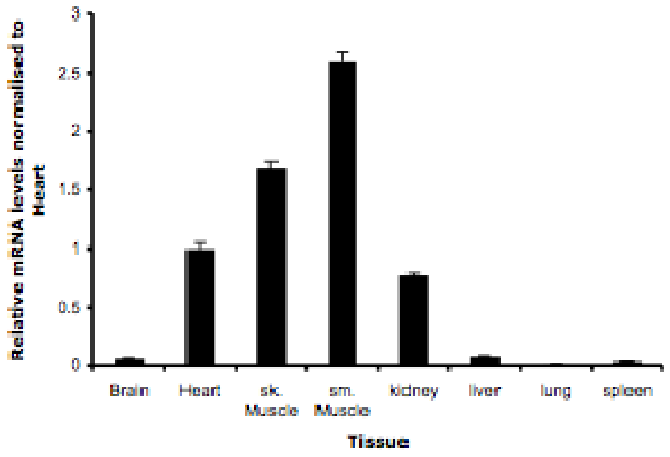
Relative mRNA levels normalised to Heart
3
2.5
2
1.5
1
0.5
0
Brain
Heart
sk. Muscle
sm. Muscle
kidney
liver
lung
spleen
Tissue

B.

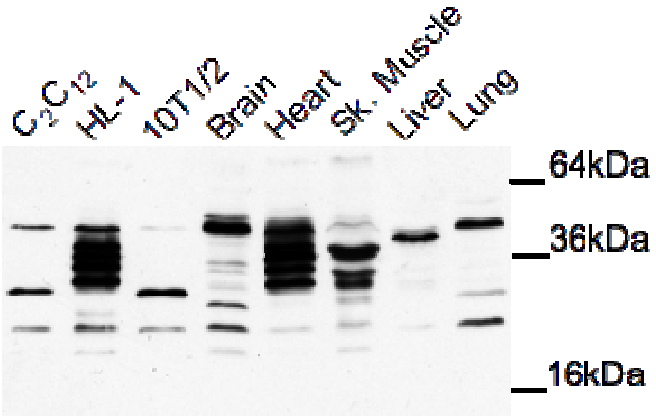
C2C12
HL-1
10T1/2
Brain
Heart
Sk. Muscle
Liver
Lung
64kDa
36kDa
16kDa

Real time PCR (qRT-PCR) data shows that MLIP is highly expressed in skeletal muscle, smooth muscle and heart tissue in mice (Figure 3A). A polyclonal rabbit anti-MLIP antibody was generated in our lab and was probed against mouse cell lines and mouse tissues depicting the different MLIP isoforms. (Figure 3B). The specificity of the MLIP antibody was validated via peptide neutralization experiments and later by stably knocking down MLIP in C2C12 cells, again revealing the specificity of the antibody. Staining of C2C12 cells and HL-1 cells (a mouse heart derived immortalized cell line) revealed that MLIP is found in the both the cytosol and nucleus of cells (Figure 4). MLIP co-localizes with LMNA in the nuclear lamina and it is seen in punctated particles. Immunofluorescent co-localization staining with a specific promyelocytic leukemia (PML) antibody and the MLIP antibody show that the punctated particles are MLIP co-localizing with PML nuclear bodies. The PML gene is involved with translocation of the RARα gene within acute promyelocytic leukemia (Zhong *et al*, 2000). The significance of this has yet to be investigated, however, PML bodies are believed to be sites of transcriptional activity and DNA replication (Stuurman *et al*. 1990). This may suggest that MLIP could play a role in transcription. MLIP is endogenously expressed in C2C12 mouse myoblast cells and is therefore used to study MLIP and its involvement in skeletal myogenesis.

Figure 4: Endogenous MLIP is localized to both the nucleus and cytosol of mouse heart derived cell line (HL-1) and mouse skeletal myoblast cell line (C2C12). A) Mouse C2C12 myoblasts were co-stained with specific polyclonal antibody for MLIP (green), LMNA (red), DAPI for DNA (blue) **B)** HL-1 were co-stained with specific polyclonal antibody for MLIP (green), LMNA (red), DAPI for DNA (blue **C)** Differentiated C2C12 cells were co-stained with specific polyclonal antibody for MLIP (green), DAPI for DNA (blue) and Myosin Heavy Chain (red). Panels A and B prepared L. Kouri and Panel B by P. Burgon.

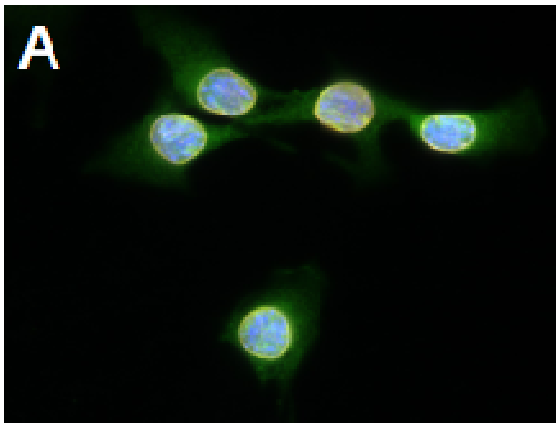
A

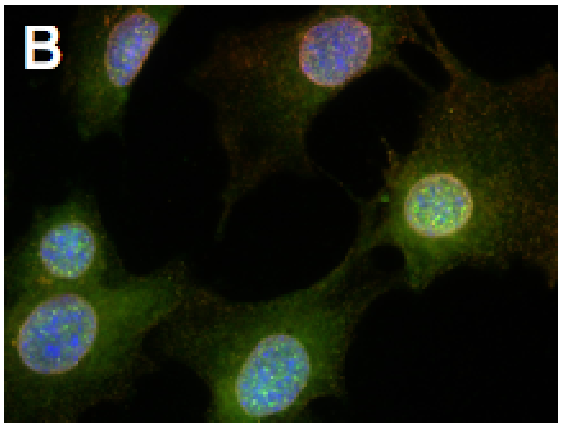
B

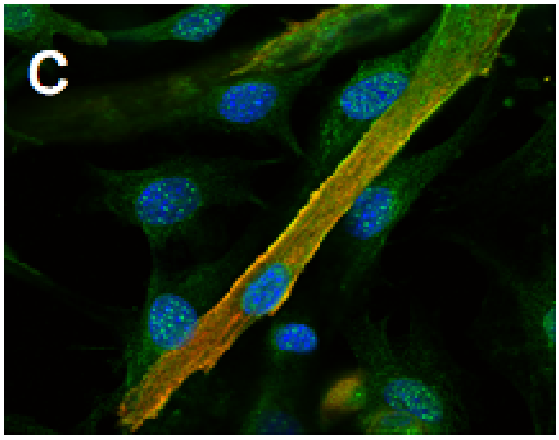
C

Figure 5. Western blot analysis of MLIP stably knocked down C2C12 cells. Western blot analysis of myogenic regulatory factors (MRFs) Myogenin and MyoD protein expression in two stably knockdown MLIP C2C12 cell lines (KD1 and KD3) at 0, 24, 48, 72, 96 and 120 hours (M, 1, 2, 3, 4,5 respectively) post-differentiation in 2% horse serum – DMEM (DM). Mouse monoclonal anti- alpha-tubulin is shown as a loading control. Myogenin and MyoD are down-regulated in stably knockdown cell lines. (Unpublished data, prepared by Elmira Ahmady).

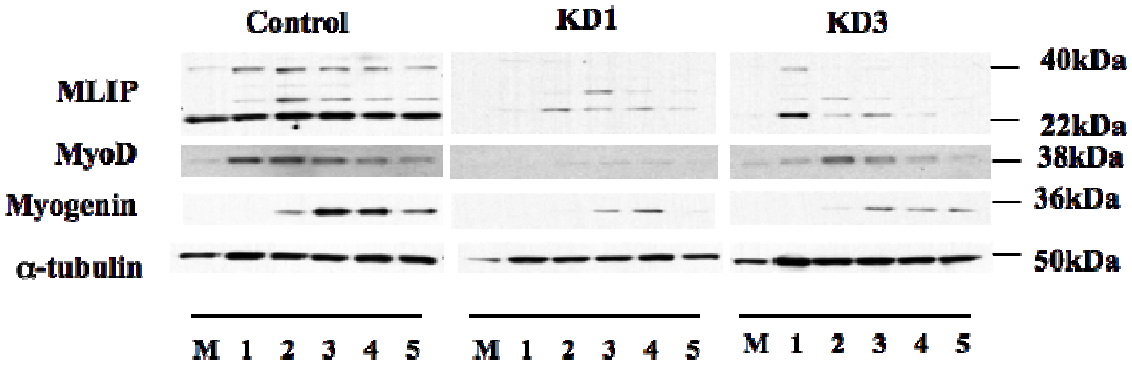
Control
KD1
KD3
MLIP
MyoD
Myogenin
α-tubulin
40kDa
22kDa
38kDa
36kDa
50kDa
M 1 2 3 4 5
M 1 2 3 4 5
M 1 2 3 4 5

Figure 6 MLIP is involved in C2C12 (mouse myoblast) cell differentiation into myotubes. Immunofluorescent images of normal C2C12 cells, pGIPZ scramble control cells and MLIP stably knockdown C2C12 cells (KD1 and KD3) were grown on gelatin coated cover slips and differentiated for 24, 72, and 120 hours (1, 3, 5 d respectively) in 2% horse serum –DMEM (DM). The stable cells were grown in the presence of 1.5µg/mL puromycin. Myosin Heavy Chain (MHC) is stained in red and nuclei were stained with DAPI (blue). Few myotubes were observed in MLIP stably knockdown cell lines (KD1 and KD3) compared to controls upon differentiation. Burgon lab (unpublished data)

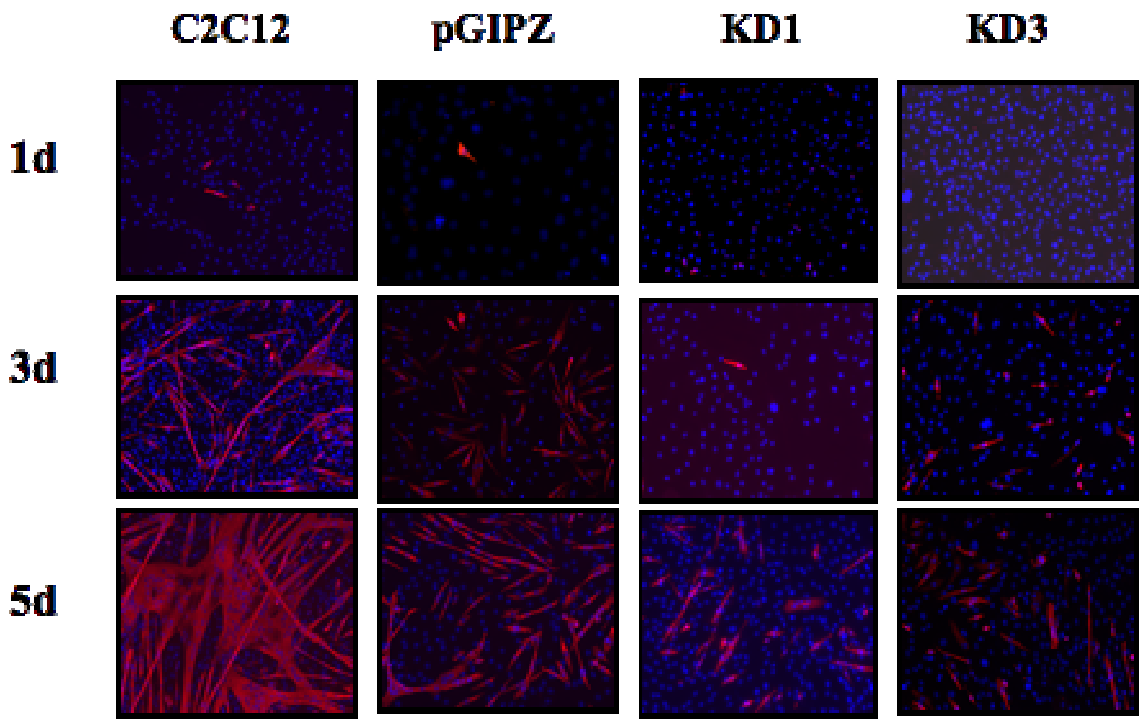
C2C12
pGIPZ
KD1
KD3
1d
3d
5d

C2C12 myoblast cells with MLIP stably knocked down (KD1) have been established using shRNA targeting the 3'UTR of MLIP. The KD1 cells show a marked reduction in differentiative capacity since few myotubes are observed (Figure 6). The KD1 cells display reduced expression levels of MRFs, specifically MyoD and Myogenin decrease relative to the C2C12 cells throughout differentiation (Figure 5). Expression of MRFs (myogenic regulatory factors) including MyoD and Myogenin are required for myotube formation (Le Grand *et al*, 2007). Chromatin immunoprecipitation (ChIP) experiments revealed that MLIP is enriched for gene ontologies associated with proliferation, differentiation and apoptosis. ChIP-on-CHIP analysis of MLIP identified key mesoderm transcription factors as putative MLIP targets, such as Six1, Six4, Six5, MEF2C, myogenin, Jun and Oct4. These factors are essential to muscle development and have been shown to be important in mesoderm cell fate and differentiation.

Objectives

To define the role of MLIP associated pathways and MLIP's involvement in muscle differentiation using the C2C12 mouse myoblast cell line.

Hypothesis

MLIP mediates the differentiation of C2C12 myoblasts into myotubes.

Specific Aims

1. To define gene expression profiles in MLIP stably knocked down C2C12 myoblasts (KD1).
2. To characterize the role of MLIP during proliferation and differentiation by using the KD1 cell line.

Chapter 2: Materials and Methods

2.1 Cell Culture Techniques

2.1.1 Growth conditions

Cells were grown in 20% FBS-DMEM growth medium containing 1% penicillin-streptomycin and additionally supplemented with 1% L-glutamine. Cells were incubated at 37°C in an atmosphere of 10% CO2.

2.1.2 Generation of stable cell lines

The stable cell lines (pGIPZ, KD1, and KD3) were generated by a previous student, Elmira Ahmady (M.Sc. thesis, University of Ottawa, 2011). In brief, C2C12 cells were transfected with three different shRNAmir constructs purchased from OpenBiosystems, using Arrest-In transfection reagent (OpenBiosystems ATR1740), in 60mm cell culture plates, which were selected in growth medium containing 1.5μg/mL of dihydrochloride puromycin (puromycin) (Sigma catalog# P8833-25MG). Media was changed daily for four weeks until clones were selected and expanded. Two MLIP-shRNAmir sequences were purchased from OpenBiosystems. These vectors were based on the design of mir-30 microRNA in the pGIPZ vector that was designed to target the 3'UTR region of MLIP. The sequences are as follows:

V2LMM_214053 **(MLIP-shRNAmir-1)**
TGCTGTTGACAGTGAGCGAGCCAACTACTTGCTAATTATAGTGAAGCCACAGAT
GTATAGTTTAGCAGTAGTTGGCCTGCTACTGCCTCGA (3'UTR).

V2LMM_211301 **(MLIP-shRNAmir-3)**
TGCTGTTGACAGTGAGCGCGCCTATAATGCCTTCTATTAATAGTGAAGCCACAG
ATGTATTAATAGAAGGCATTATAGGCTTGCCTACTGCCTCGGA (3'UTR).

The vectors were transformed into DH5α bacterial cells and were spread onto ampicillin positive agar plates and incubated overnight in a 37^{o}C incubator. Colonies were picked and grown in LB broth containing 50μg/mL ampicillin overnight at 37^{o}C at 250rpm.

DNA minipreps were then performed according to the standard phenol-chloroform alkaline lysis plasmid DNA miniprep protocol. DNA concentrations were determined using NanoDrop Spectrophotometer ND-1000.

2.1.3 Generation of new stably knocked down MLIP cells via shRNA (pGIPZ-A, KD1-A, KD3-A)

These stables were generated using the same vectors as previously done (See Section 2.1.2) except that colonies were not selected. In brief, C2C12 cells were transfected with three different shRNAmir constructs purchased from OpenBiosystems using Lipofectamine2000 transfection reagent (Invitrogen catalog # 11668-019) in 60mm cell culture plates were selected in growth medium containing 1.5µg/mL of puromycin (Sigma catalog# P8833-25MG). Media was changed daily for four weeks until cells were confluent and expanded.

2.1.4 Transient transfections with pcDNA3.1-Control and MLIP expression vector

Transient transfections using pcDNA3.1-Control vector and pcDNA3.1 expressing exons 1, 2,3 7,8,9 of the *MLIP* gene (pcDNA3.1-MLIP) into the pGIPZ and KD1 cell lines were done so using Fugene6 or Lipofectamine2000 transfection reagents, as per manufacturer's protocol. Briefly, once the cells were 50% confluent, they were transfected with either the control vector or the MLIP expression vector in serum-free and antibiotic free media. The cells were incubated for 6 hours at 37^{o}C. The media was replaced with normal growth media (GM) and the cells were put back into the 37^{o}C incubator for 24hours. Following this, differentiation was inducing by removal of GM and replacement with differentiation media (DM), which contains 2% horse serum. Cells were harvested and lysed for immunoblotting (refer to Section 2.3.1 and 2.3.3).

2.2 Determination of the proliferation rate of MLIP knockdown

To determine the rate of proliferation of the KD1 cell line compared to the pGIPZ control and C2C12 cells, approximately 16,000 cells were seeded onto 60mm plates and were incubated at 37°C. The growth medium was replaced every second day. Throughout the course of a week, a plate from each cell line was removed, trypsinized to detach the cells from the plates and were neutralized with soybean trypsin inhibitor (Sigma, catalog # T6522). The cells were pelleted by spinning at 3000rpm for 5min and where re-suspended in DMEM. The cells were counted using the Vi-Cell Cell Viability Analyzer (Beckman Coulter). Images of the cells were taken prior to trypsinization using an Olympus CKX41 Inverted light microscope to visualize the cells.

2.3 Whole cell extract preparation and Western Blotting

Cells were lysed with Complete NP-40 Lysis Buffer (50mM Tris-HCl pH8, 200mM NaCl, 20mM NaF, 20mM β-glycerolphosphate, 0.5% NP-40) for which 10mL was supplemented with 1 Complete Mini Protease Inhibitor Cocktail tablet (Roche 11836153001), 1 PhosphoStop Phosphatase Inhibitor Cocktail tablet (Roche catalog# 04906837001), 0.1mM Na3VO4, and 1mM DTT. Lysates were incubated for 20 min on ice where samples were vortexed every 5-10 min. Samples were then spun at 10,000g for 10 min and supernatants were transfered to new 1.5ml microcentrifuge tubes. Total protein was quantified using Bio-Rad Protein Assay using Bio-Rad Protein Assay Dye Reagent Concentrate (Bio-Rad catalog # 500-0006). Lysates were stored at -80°C until ready for use.

Western blots were run using 20µg of total protein lysate, which was loaded into 1mm-thick 12% gels or 4-15% gradient gels (BioRad catalog# 456-1086) and run at 200 V for 30min in the presence of Tris-based running buffer. The SeeBlue Plus2 Pre-Stained

Standard (Invitrogen catalog# LC5925) was used as a protein marker. The samples were then transferred onto PVDF membranes for 1 hour at 100V in 20% Methanol Tris-Glycine transfer buffer. Blots were incubated for 1 hour on a shaker at room temperature in 5% skim milk–TSBT (0.1% Tween20). Blots were washed in TBST (0.1% Tween20) followed by primary antibody incubation overnight at 4°C on a shaker (See Section 2.3.2 for details).

2.3.1 Coomassie Blue staining of 4-15% gradient gels

To demonstrate equal loading of protein samples, 10 µg total protein was loaded onto 4-15% gradient gels and were run for 30 min at 200V (refer to Section 2. 3). The gels were stained and destained following the standard staining methods using Coomassie Blue solution. Images of the gels were taken to show equal loading of protein samples.

2.3.2 Protein expression detection during C2C12 cell differentiation

C2C12 cells were grown to ~60% confluency and forced to differentiate by withdrawal of GM and replacing with differentiation media (DM) which contains 2% horse serum (HS) (instead of 20% FBS). Cells were harvested when in an undifferentiated state, 24 hours, and 48 hours post-differentiation. Cells were lysed and lysates were immunoblotted as previously described (refer to Section 2.3).

For detection of MLIP, a rabbit anti-MLIP antibody was developed in-house and used at a concentration of 1:50,000 in all Western blots. The antibody specificity was previously validated via peptide neutralization experiments and transient knockdown experiments done in C2C12 cells by prior students. Note that all primary and secondary antibody incubations were done in 5% skim milk-TBST (0.1%Tween20) where the primary antibody incubations were done on a shaker overnight at 4°C. An anti-Myogenin 5FD antibody (Santa Cruz catalog# sc-52903) was used at a dilution of 1:1000, a goat polyclonal

anti-Lamin A/C (N-18) (Santa Cruz catalog# sc-6215) was used at a dilution of 1:500, and a mouse monoclonal anti-α-tubulin (clone DM1A, ascites fluid) antibody (Sigma catalog# T9026) was used at a dilution of 1:5000.

The secondary antibody incubations were done at room temperature for 1 hour on a shaker. The secondary antibodies that were used are anti-rabbit IgG HRP-linked antibody (Cell Signaling catalog# 7074), anti-mouse IgG, HRP-linked antibody (Cell Signalling catalog# 7076), and anti-goat IgG HRP-linked antibody) (Santa Cruz catalog# sc-3854). These were used at the following dilutions: 1:2000, 1:3000, and 1:2000, (respectively). This was followed by 5min incubation with SuperSignal West Pico Chemiluminescent substrate (ThermoScientific catalog# 34080) as per manufacturer's protocol. Blots were then exposed onto autoradiography film (Fisher Scientific catalog# PI-34093).

2.4 Isolation of total RNA from cells

C2C12, pGIPZ and KD1 cells were grown to 60% confluency in 100mm plates and total RNA was isolated as per RNAprep - TRIzol combined with Columns protocol (Untergasser, 2008). In brief, cells were washed with 1xPBS and lysed with 500 µl of TRIzol Reagent (Invitrogen catalog# 5596-018) followed by incubation for 5 min at room temperature in a 1.5ml microcentrifuge tube. One hundred microliters chloroform was added and incubated for 2 min at room temperature. Samples were spun down at 12,000 g for 15 min at 4°C and the upper phase was transferred to a sterile RNase-free microcentrifuge tube upon which 300µl of 70% ethanol was added and mixed well. Samples were transferred to RNeasy Mini spin column (RNeasy Mini Kit QIAGEN catalog# 74104) and were centrifuged for 15 s at 8000g at 4°C. Note that the flow-through was discarded after every centrifugation step. Seven hundred microliters of Buffer RW1 was added and then spun

down for 15 s at 8000g followed by the addition of 500µl of Buffer RPE. The 15 s centrifugation and the addition of RPE were done twice. The columns were spun for an additional 2 min at 13, 200 rpm to dry the columns and then placed into a sterile RNase-free 1.5mL microcentrifuge tube. Thirty microliters of RNase-free water was added to each column and incubated for 2 min at room temperature and centrifuged for 1 min at 13, 200rpm to elute the RNA. Samples were stored at -80°C. RNA samples were analyzed via the BioAnalyzer 2100 (Agilent G2940CA) following manufacturer's instructions.

After RNA was isolated, the samples were then DNase-treated using the Promega RQ1 RNase-Free DNase kit (Catatlog# M6101) according to manufacturer's recommendation.

2.5 Quantitative Real-Time PCR (qRT-PCR)

RNA was isolated then DNase-treated using the Promega RQ1 RNase-Free DNase kit (Cat.# M6101) according to manufacturer's recommendation. One microgram of treated total RNA (refer to Section 2.9.1 for RNA isolation protocol) was used for the generation of complementary DNA (cDNA), using M-MulV Reverse Transcriptase (NEB catalog# M0253S) according to the First Strand Synthesis Protocol. Note that oligo dT primers were used in the RT-PCR reactions instead of random primers.

Complementary DNA transcripts were quantified by relative qRT-PCR using the Roche LightCycler® 480 Multiwell PCR System, the LC480 machine and the LightCycler® 480 SYBR Green I Master kit (Catalog# 0470751600), as per manufacturer's indication. Real-time PCR experiments were realized using 96-well PCR plates (Catalog# 04729692001). Reaction mix was halved to 10µL with: 1.5µL PCR-grade water, 0.5µL Forward and Reverse PCR primer (5µM), 5µL 2X concentrated Master Mix, and 2.5µL

cDNA (diluted 1:5 ratio in RNase free water). Table 2 provides a list of primers used in the experiments.

The Ct values were interpreted using relative expression analysis employing the $\Delta\Delta C_T$ method. This was used to determine the fold change of a given gene in the KD1 cells relative to the controls (C2C12 and pGIPZ), and was then normalized to GAPDH expression (n=3). This was done experimentally three times.

Table 2 qRT-PCR primers used in experiments.

Gene	Primer Sequence
EGR3	F: 5' CCGGTGACCATGAGCAGTTT-3'‘ R: 5'-TAATGGGCTACCGAGTCGCT-3'
PITX2	F: 5'-GGAATGGAGACCAATTGTCGC-3' R: 5'-CGCCTAATTGCACGCAGG-3'
PAX7	F: 5'-CTCAGTGAGTTCGATTAGCCG-3' R: 5'-AGACGGTTCCCTTTGTCGC-3'
TBX3	F: 5'-AGATCCGGTTATCCCTGGGAC-3' R: 5'-CAGCAGCCCCCACTAACTG-3'
LEF1	F: 5' TGTTTATCCCATCACGGGTGG R: 5'-CATGGAAGTGTCGCCTGACAG
HDAC3	F: 5'-ACCGTGGCGTATTTCTACGAC-3' R: 5'-CAGGCGATGAGGTTTCATTGG- 3'
RXRα	F: 5'-TGCGTCACTAGAAGCGTACTGCAA-3' R: 5'-GCTTGAAGAAGAACAGGTGCTCCA-3'
GLIS3	F: 5'-CATTTTCGCCAGCAATCATTCA-3' R: 5'-AGTGGAGGTAACTGGGAGGAG-3'
GAPDH	F; 5'-GTGAAGGTCGGTGTGAACG-3' R: 5'-ATTTGATGTTAGTGGGGTCTCG-3'
Oligo dT	5'-TTTTTTTTTTTTTTTTTTTT-3'

2.6 Immunofluorescence Microscopy

2.6.1 Slide Preparation

Under sterile conditions, autoclaved cover slips were placed into the wells of a 12-well plate and coated with 0.02% gelatin and incubated in a 37°C incubator for 30min, after which the excess gelatin was aspirated from the wells. Cells were seeded onto the cover slips at appropriate dilutions for the specific experiments. After completion of experimental

treatments, cover slips were washed thrice with PBS and incubated in pre-chilled 100% methanol for 20 min on ice to fix the cells. Methanol was aspirated and cover slips were washed three times with PBS. At this point cover slips were either stored at 4°C in PBS until ready to stain or continued on with staining. Cover slips were placed into a clean 12-well plate followed by incubation with anti-MLIP (1:10 000 dilution dissolved in 1.5% FBS/PBS for 1 hour at room temperature. Note that to identify myotubes and the presence of terminal differentiation, cover slips were also incubated with anti-MHC (MF1) antibody (Developmental studies hybridoma bank) at 1: 20 dilution for 1 hour at room temperature in 1.5% FBS/PBS solution. Cover slips were washed with PBS followed by incubation with fluorescent-conjugated secondary antibody at 1:1000 dilution (Alexa Fluor 568 goat anti-rabbit IgG (molecular probes), Regulus Red 594 anti-mouse IgG (LP Bio CA-0251-250) in the dark for one hour. To stain the nuclei, cover slips were washed in PBS and were stained with DAPI (1µg/ml) for 3 min protected from light. Cover slips were washed three times in PBS and mounted onto slides using fluorescent mounting media (DAKO s3023) and were allowed to dry overnight before visualization under the Zeiss Fluorescent Microscope (Dr. Alex Stewarts Laboratory, Heart Institute).

2.7 Exon Microarray Analysis

2.7.1 GeneChip® Whole Transcript (WT) Sense Target Labeling Assay

The GeneChip WT Sense Target Labeling kit (Affymetrix catalog# 900671) was used to reduce and label 1µg of total RNA (refer to Section 2.4) (as per manufacturer's protocol) from C2C12, pGIPZ and KD1. The reduced, fragmented and labeled products were hybrizided onto GeneChip Mouse Exon 1.0 ST Array (Affymetrix catalog# 900819) as per manufacturer's protocol (n=3).

2.7.2 GeneChip® Expression Wash, Stain and Scan User Manual

The fluidics stations in the Ruddy centre at the University of Ottawa Heart Institute were used as per manufacturer's protocol with the assistance from Dr. Alexandre Stewart's lab technicians. The Fluidics Station 450 was used following FS450_0001 fluidics protocol and the FS450_0001 fluidics script protocol.

2.7.3 Exon Microarray Analysis and Quality Control (QC)

Affymetrix Expression Console software was used to look conduct QC assessments of the microarrays. Quality controls include the following tests: 1) Labeling controls whereby Lys<Phe<Thr<Dap; 2) Signal Histogram; 3) Pearson's Correlation for RMA Core, PLIER Core, Controls, and RMA Extended; 4) Log Expression Signal; 5) Relative Signal Box Plot; 6) Relative Log Expression Signal; 7) Box Plot of Probe Cell Intensity; 8) Relative Probe Cell Intensity; 9) External Spike Controls whereby BioB<BioC<BioD<Cre; 10) Samples are within bounds and no outliers were present.

Exon microarrays were analyzed using Partek Genomics Suite software (provided by Dr. Ed O'Brien) where the data was first normalized via RMA normalization (recommended by Affymetrix) followed by Tukey's post-test. Then data was analyzed via the 1-way ANOVA contrast analysis comparing each group to the other (ie. KD1 vs C2C12, KD1 vs pGIPZ, and pGIPZ vs C2C12). Data with a p-value of <0.05 was considered significant.

2.8 Statistical Analysis

Results were analyzed with student t-test (except where indicated) and a P-value of < 0.05 was considered significant.

2.9 Database for Annotation, Visualization and Integrated Discovery (DAVID) analysis

DAVID is an online database sponsored by the NIH that was used to further interpret the array data following online directions (Huang DW *et al*, 2009).

2.10 Animals

All animal studies were performed in accordance with the policies and guidelines of the University of Ottawa Animal Care Committee.

2.10.1 Generation of an *in vivo* Cre-CMV MLIP$^{+/-}$ heterozygote mouse model

The conditional MLIP knockout mouse was produced at the University of Connecticut Gene Targeting and Transgenic Facility and it arrived at the University of Ottawa Heart Institute in October 2009. Briefly, the strategy was to insert loxP sites ~1kb 5' of the transcriptional start site of MLIP in a poorly conserved genomic region and a second loxP sequence within a poorly conserved region of the first intron of MLIP (Supplemental Figure S9). This was done so that upon Cre-recombinase mediated recombination, the MLIP putative transcriptional start site, the proximal promoter and exon1 would be excised {Mouse chr9: 77,194,851-77,200,893} (Supplementary Figure S9).

2.10.2 Echocardiographic Analysis

Echocardiography was performed with a Hewlett Packard Sonos 4500 ultrasound machine and a 6-15 MHz linear array transducer on anesthetized mice, with a heart rate greater than 450 bpm, as previously described (Fatkin *et al*., 2000).

Chapter 3: Results

3.1 Gene level analysis of C2C12, pGIPZ and KD1 cell lines using Exon Microarrays

Our lab has previously shown that stably knocked down MLIP protein expression in C2C12 cells down-regulates both MyoD and myogenin expression levels (Figure 5). This also causes a reduction in the number of myotubes generated upon being stimulated to differentiate (Figures 6). To determine the signaling pathways associated with MLIP levels, gene expression profiling experiments were performed. In brief, total RNA was isolated from C2C12, pGIPZ and KD1 cells and was reduced to only messenger RNA (mRNA) using the GeneChip WT Sense Target Labeling kit. This was followed by a series of PCR reactions where the final PCR products were fluorescently labeled and hybridized onto GeneChip Mouse Exon 1.0 ST Array from Affymetrix. The microarrays were washed and scanned using Affymetrix Fluidics Station 450, following the FS450_0001 fluidics protocol and the FS450_0001 fluidics script protocol. The microarray data was normalized using RMA normalization. This was followed by 1-way ANOVA analysis and by Tukey's HD statistical test, to compare the three cell lines amongst one another (ie. KD1 versus C2C12 cells, KD1 versus pGIPZ cells, and pGIPZ versus C2C12 cells). Note that only gene level expression analysis was performed. This was done in-house three times from three independent vials of cells. A total of 16 715 genes were analyzed on the arrays and only those with a p-value of 0.05 or less were deemed statistically significant (n=3). Table 2 depicts the total number of significant genes and demonstrates the percentage of genes up-regulated versus those that are down-regulated, when comparing the KD1 to the controls.

When examining KD1 gene expression relative to C2C12 cells, there was a statistically significant difference between the numbers of up-regulated genes versus down-regulated ($p=0.0001$). Of the 754 differentially regulated genes identified, 298 of those

genes were up-regulated (approximately 40%) and 456 of the genes were down-regulated (Table 3). When looking at KD1 gene expression compared to pGIPZ gene expression, the differences between up-regulated and down-regulated gene expression was significant (p=0.0001). From a list of 547 differentially regulated genes, 194 genes were up-regulated (approximately 35%) and the remainder were down-regulated (approximately 65%) (Table 3). Upon comparing KD1 to both controls, the percentage of genes that were up-regulated versus those that were down-regulated is fairly similar. A comparison of the controls shows that 1121 genes were differentially regulated, however this difference was not significant in terms of up-regulated versus down-regulated genes (p=0.7881). Thus, knocking down MLIP protein levels differentially affects gene level expression.

Table 3:Statistically significant, differentially regulated genes post 1-way ANOVA contrast analysis examining normal C2C12 cells, pGIPZ scramble control, and the MLIP stably knockdown cell line KD1 (n=3).

	Total Genes (p<0.05)	Up-regulated Genes	% Up-regulated Genes	Down-regulated Genes	% Down-regulated Genes	p-value (Chi-squared test)
KD1 vs C2C12	754	298	39.52	456	60.48	0.0001
KD1 vs pGIPZ	547	194	35.47	353	64.53	0.0001
pGIPZ vs C2C12	1121	565	50.40	556	49.60	0.7881

Given that knocking down MLIP protein levels causes differentially regulated genes, we attempted to denote functional meaning to the affected genes. To do this, we used an online database (that is sponsored by the NIH) known as the Database for Annotation, Visualization, and Integrated Discovery (DAVID), to assert the functionality of the selected genes. Analysis of the gene expression data revealed that amongst the differentially regulated genes in KD1 versus C2C12, 131 of the 794 genes are transcription factors/regulatory factors (TF) (p=0.0001), which represents 17% (Table 4). Seventy percent

of the TFs were down-regulated whereas only 30% of the TFs are up-regulated (p=0.0001). When comparing the KD1 cell line to the pGIPZ cell line, only 49 genes are TFs, which is less than 10% of the 547 differentially regulated genes. Almost 60% of the TFs are down-regulated (Table 4). There are far fewer transcription factors changing in the KD1-vs pGIPZ category compared to the KD1 vs C2C12 category. Comparison of the controls shows the 172 differentially regulated genes are TFs and that over 60% of those TFs are down-regulated (p=0.0061). Thus, knocking down MLIP protein expression in C2C12 cells affects expression of TFs where the majority of the targeted genes are down-regulated. Since a large number of TFs are affected by stably knocking down MLIP, we decided to select a group of them for validation purposes.

Table 4 Transcription factors (TFs) that are differentially regulated in KD1, pGIPZ, and C2C12 cells (n=3).

	Total number of TFs	Number of Up-regulated TFs	Number of Down-regulated TFs	%Up-regulated	%Down-regulated	P-value (Chi-squared test)
KD1 vs C2C12	131	39	92	29.77	70.23	0.0001
KD1 vs pGIPZ	49	20	29	40.82	59.18	0.1985
pGIPZ vs C2C12	172	68	104	39.53	60.47	0.0061

3.1.1 Validation of transcription factors affected by the knockdown of MLIP expression

Transcription factors (TFs) were chosen from the KD1 vs C2C12 cell analysis for validation of the microarrays using real time PCR (qRT-PCR). Figure 7 depicts the fold changes of the TFs found on the microarrays. The vast majority of genes were down-regulated due to the knockdown of MLIP. These TFs are associated with proliferation, differentiation and cell cycle progression and thus are used as a starting point for analysis.

Real time PCR (qRT-PCR) was used to study the expression of 8 of the listed TFs in the KD1 cells relative to the controls (C2C12 and pGIPZ cells). Relative expression analysis using the $\Delta\Delta C_T$ method was used to determine the fold change of a given gene in the KD1 cells relative to the controls (C2C12 and pGIPZ), and was then normalized to GAPDH expression (n=3). GAPDH expression was constant in all three cell lines making it an appropriate housekeeping gene. Eight of the 13 TFs shown in the fold change graph (Figure 8) were studied. When comparing KD1 to C2C12 cells, *HDAC3*, *TBX3*, *LEF1*, *PAX7*, *RXRA*, *PITX2*, and *EGR3* were all down-regulated, this is in accordance with the microarrays. On the other hand, *GLIS3* should have been up-regulated by approximately 30%, rather it was slightly down-regulated by approximately 20% compared to C2C12 cell expression.

When these selected genes were normalized to pGIPZ expression (ie. KD1 gene expression normalized to pGIPZ expression), all of the genes were up-regulated (with the exception to *PITX2*, which showed a slight decrease in expression) instead of being down-regulated. *PAX7* showed an approximate 5.5-fold increase in expression compared to the 2-fold decrease seen in the microarrays. The difference in expression between controls compared to the KD1 cell line suggests that future studies should be done using different target genes.

Figure 7 Selection of transcrition factors that are differentially regulated upon knockdown of MLIP expression as revealed by exon microarray analysis. One-way ANOVA analysis followed by Tukey's post-hoc test, looking at the fold change of selected transcription factors. These transcription factors are involved in cellular regulation, proliferation and differentiation. Only 13 of 131 transcription factors are shown (n=3).

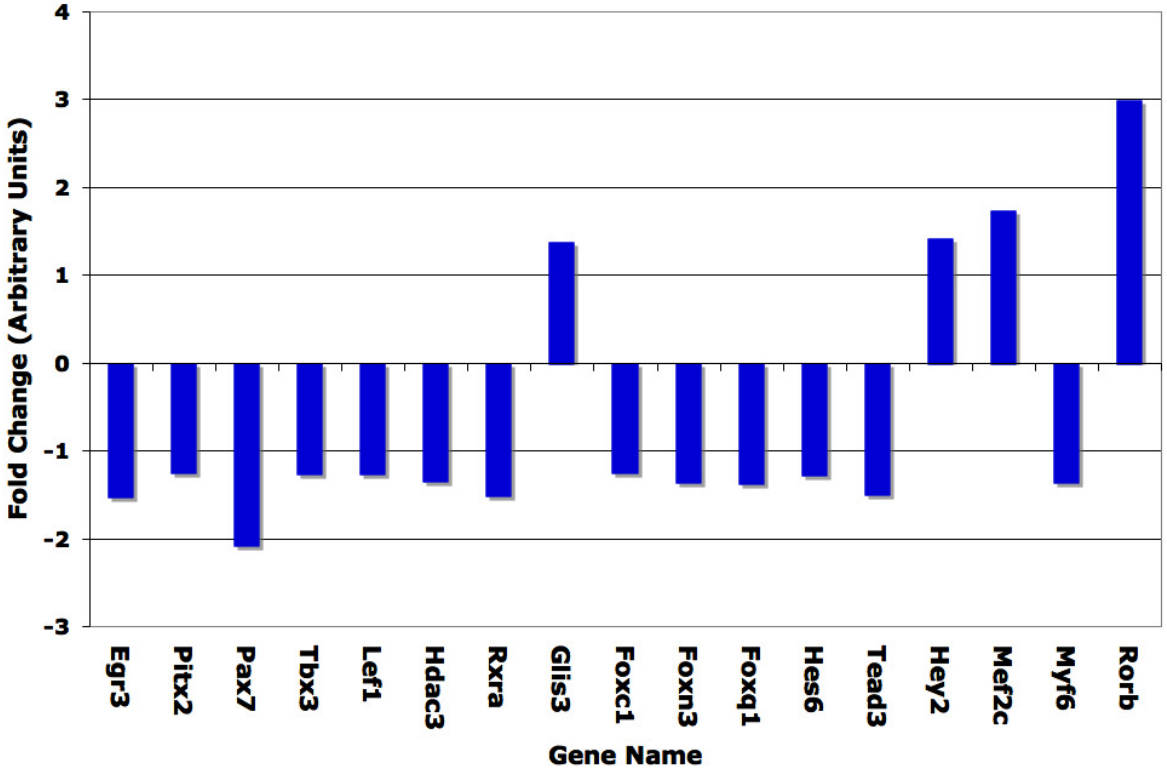
Fold Change (Arbitrary Units)
4
3
2
1
0
-1
-2
-3
Egr3
Pitx2
Pax7
Tbx3
Lef1
Hdac3
Rxra
Glis3
Foxc1
Foxn3
Foxq1
Hes6
Tead3
Hey2
Mef2c
Myf6
Rorb
Gene Name

Figure 8 Transcription factors affected by MLIP knockdown. Real time PCR (qRT-PCR) validations of transcription factors that are differentially regulated upon MLIP knockdown. Transcription factors were used to validate the exon microarrays. The graphs show the expression of the TFs in the KD1 cell line relative to the control cells (pGIPZ and C2C12 cells) normalized to GAPDH expression (the housekeeping gene) as calculated by relative quantification (using the $\Delta\Delta C_T$ method) (n=3).

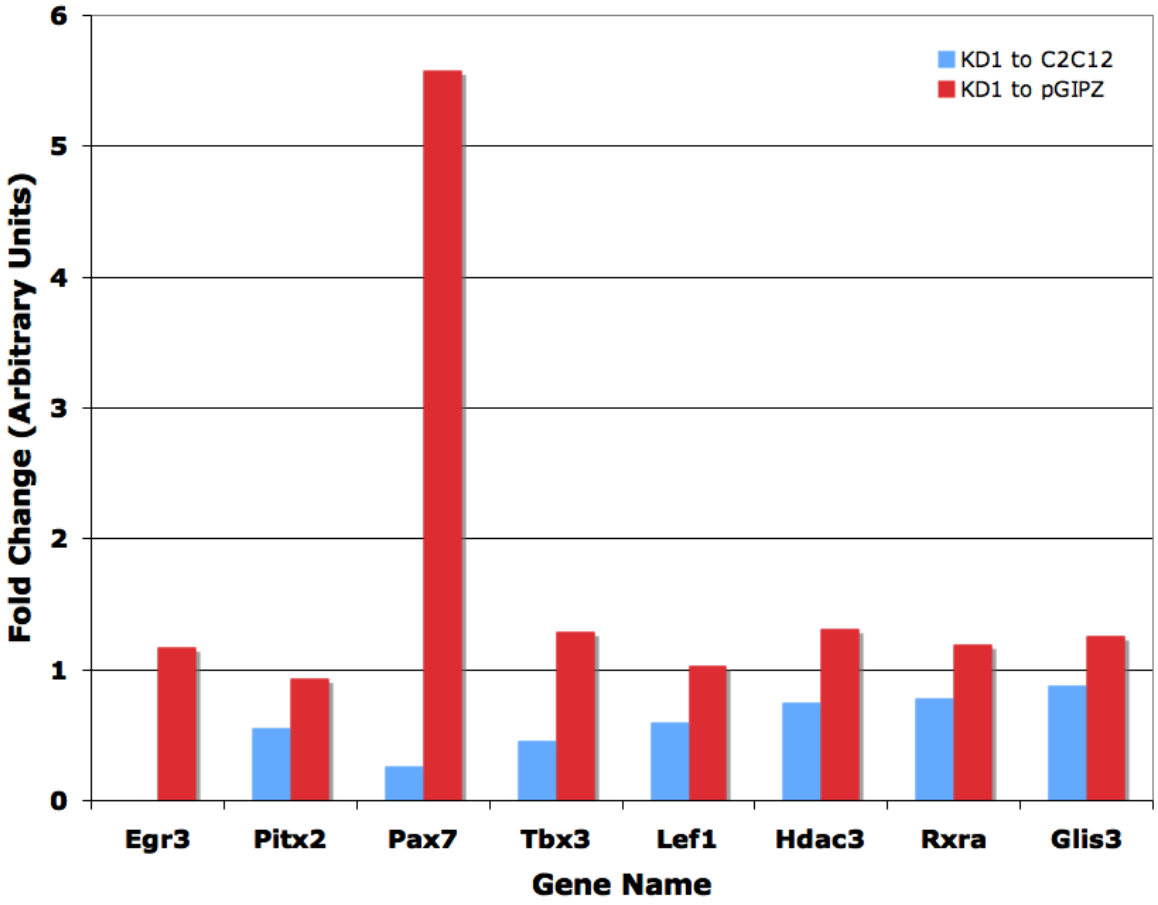
KD1 to C2C12
KD1 to pGIPZ
Fold Change (Arbitrary Units)
0
1
2
3
4
5
6
Egr3
Pitx2
Pax7
Tbx3
Lef1
Hdac3
Rxra
Glis3
Gene Name

3.1.2 Selecting gene targets for investigation

Given the discrepancies found between the normal C2C12 myoblast cells and the pGIPZ cells, we decided to take a different approach to analyzing the microarrays. To do this we stratified all three gene lists from the different cell line comparisons (ie. KD1 vs C2C12, KD1 vs pGIPZ, and pGIPZ vs C2C12 cells) and grouped them using a Venn diagram, based on the presence or absences of similar genes (Figure 9). This produced seven different groups, where we chose to focus on genes that were only identified in the KD1 vs pGIPZ comparison. This yielded 166 genes from the KD1 vs. pGIPZ comparison that were used for further analysis (Table 5). Thus, 166 differentially affected genes out of a total of 547 genes were entered into the DAVID database to categorize them based on any associated disease phenotypes and biological processes.

Figure 9: Venn diagram of the differentially affected genes in KD1, pGIPZ, C2C12 cell lines All statistically significant genes from all three comparisons (based on the 1-wasy ANOVA contrast analysis) were categorized into the venn diagram.

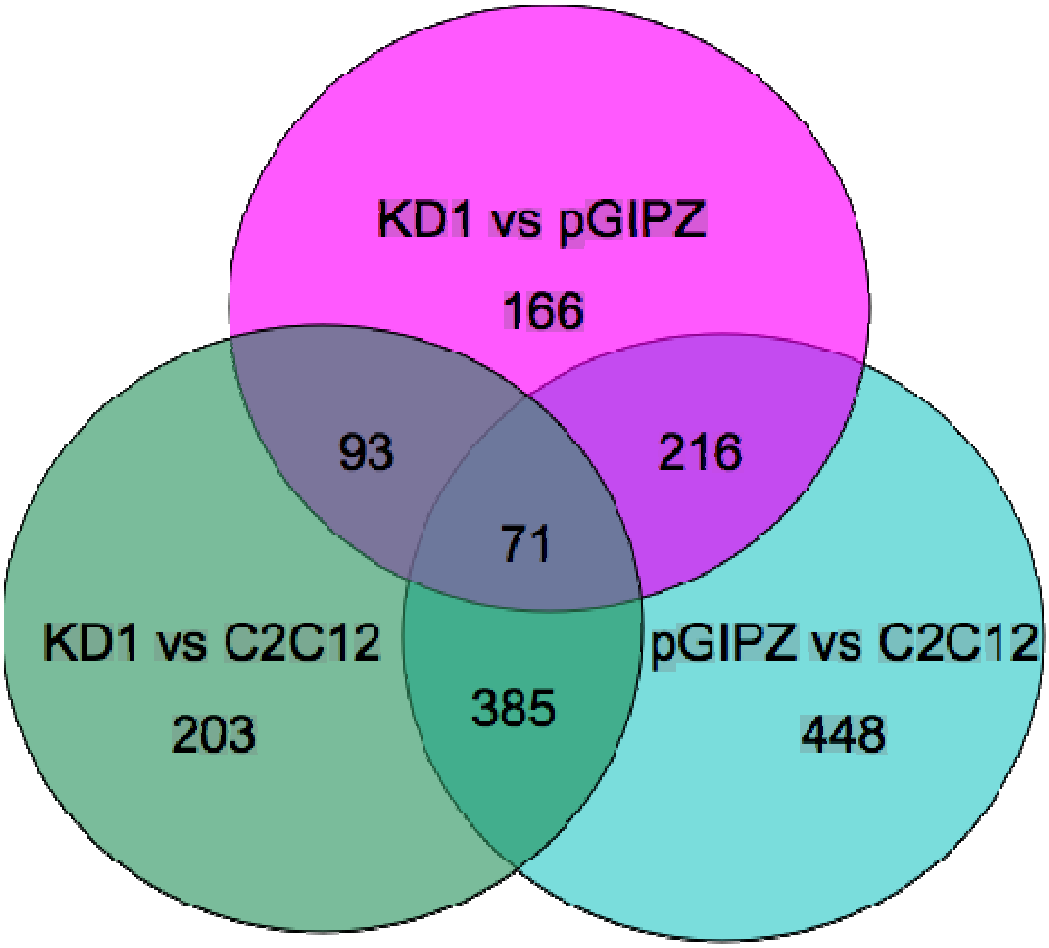
KD1 vs pGIPZ
166
93
216
71
KD1 vs C2C12
203
385
pGIPZ vs C2C12
448

Table 5: The 166 genes as identified in the Venn diagram (Figure 9).

2310057N15Rik	Defb14	Marveld2	Sgcd
2510048L02Rik	Defb21	Mmab	Sh2d1a
2610318N02Rik	Dmpk	Mtg1	Smpdl3a
9230105E10Rik	Dnaja2	Mug1	Snx8
A330021E22Rik	Dnajb7	Myef2	Srgap3
A830093I24Rik	Dok4	Ndst3	Srp9
AA881470	Dsg1c	Nefl	Steap1
Aacs	Dtx2	Nsg1	Stk11ip
Abhd8	EG329763	Olfr1043	Stk36
Abo	Eya1	Olfr1125	Stx2
Adarb1	Fam115a	Olfr1167	Tcp10b
Adck5	Fgf5	Olfr1413	Tcta
Agfg2	Gpm6b	Olfr1454	Thbd
Ahdc1	Gpr19	Olfr285	Tmem14a
Aim1	Gpr75	Olfr292	Tmem86a
Ano5	Gpx8	Olfr320	Tnp1
Arhgdig	Grpr	Olfr345	Trappc5
Athl1	Gtf2ird2	Olfr44	V1rc15
Azgp1	Hcrt	Olfr491	V1rc17
B4galt3	Hectd3	Olfr683	V1rd18
Bcl2	Hmga2	Olfr774	V1re9
Bmpr1b	Hnmt	Olfr790	V1rh8
C630028N24Rik	Hspb8	Olfr887	Vmn2r48
Camk2d	Idh2	Olfr895	Vps33a
Capn10	Il10	Osbpl3	Vsig4
Cc2d1a	Il1f9	Oxr1	Wisp1
Ccr5	Il1rl1	Pcdhb15	Xpc
Cd248	Impg2	Pde2a	Yod1
Cd2bp2	Jak2	Pemt	Ywhag
Cmtm3	Kptn	Phldb2	Zfat
Cnot1	Krtap6-2	Pkp1	Zfp212
Cntnap4	Lce1g	Plcb1	Zfp330
Cobll1	Lcn5	Podxl	Zhx2
Coro1c	Lhfpl1	Ppap2b	Zkscan5
Cpne2	Lipf	Ppp1r3c	
Csn3	Lmnb2	Ppp2r2b	
Csrnp1	Lrrc16a	Ptpdc1	
Cst6	Lrrc61	Rbpms2	
Cxadr	Lrrc68	Rdh1	

3.1.3 Knocking down MLIP expression affects genes implicated in diseases

Using DAVID, 30 genes out of 166 genes were identified that are linked to diseases (Supplemental Table S2). Of the 30 genes, five genes are directly associated with laminopathies, myopathies, and neuropathies (Table 6). Figure 10 shows the fold changes for these selected genes according to the microarrays. *DMPK*, *HSPB8*, and *LMNB2* all show decrease gene expression whereas *NEFL* and *SGCD* are both up-regulated. Mutations of *DMPK* and *SGCD* can cause myopathies; mutations of *LMNB2* cause Acquired Partial Lipodystrophy (APL), which is a laminopathy; and mutations of *NEFL* and *SGCD* both cause CMT and LGMD (respectively) (Table 6). In summary, knocking down MLIP expression affects genes that are directly linked to laminopathies, myopathies, and neuropathies.

Table 6 Genes associated with myopathies, neuropathies and laminopathies .

Gene	Gene Name	OMIM_DISEASE	Classification
Dmpk	dystrophia myotonica-protein kinase	Dystrophia myotonica (DM) 1	Myopathy
Hspb8	heat shock 22kDa protein 8	Charcot-Marie-Tooth disease, type 2L Neuropathy, distal hereditary motor, type II Neuropathy, distal hereditary motor, type IIA,	Neuropathy
Lmnb2	lamin B2	Acquired Partial Lipodystrophy	Laminopathy, (Lipodystrophy)
Nefl	neurofilament, light polypeptide	Charcot-Marie-Tooth disease, type 1F Charcot-Marie-Tooth disease, type 2E	Neuropathy
Sgcd	δ-sarcoglycan (35kDa dystrophin-associated glycoprotein)	Cardiomyopathy, dilated, 1L Limb-girdle Muscular dystrophy, type 2F	Myopathy

Figure 10: Gene expression of targets regulated by the knockdown of MLIP that are linked to diseases. Fold changes of selected genes as determined by the exon microarrays, post gene-level analysis (n=3). Refer to Table 6 for the phenotype descriptions.

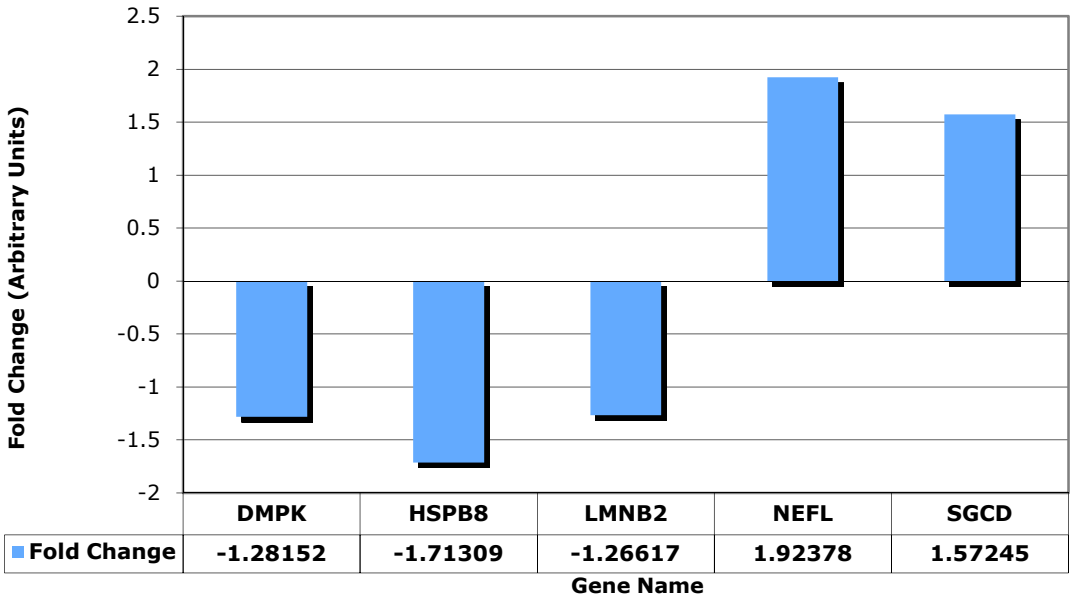
Fold Change (Arbitrary Units)
2.5
2
1.5
1
0.5
0
-0.5
-1
-1.5
-2
DMPK
HSPB8
LMNB2
NEFL
SGCD
Fold Change
-1.28152
-1.71309
-1.26617
1.92378
1.57245
Gene Name

3.2 Knockdown of MLIP protein expression via shRNA does not affect the rate of proliferation

To determine if MLIP affects the growth rate of C2C12 cells, approximately 16,000 cells of the knockdown cell line (KD1) and the control cells (pGIPZ, and wild type C2C12 cells) were seeded onto 60mm plates and were grown under normal growth conditions (in the absence of puromycin) (n=3). The cells were permitted to grow without intervention throughout the course of a week and images were taken daily using an Olympus CKX41 Inverted light microscope in order to document any morphological changes (n=3). The cells were then trypsinized using 0.05% trypsin-EDTA and neutralized with soy bean trypsin inhibitor and counted using a Vi-Cell Cell Viability Analyzer (Beckman Coulter) (Figure 11). All three cell lines appear to be growing at the same rate until Day 5, where cell growth plateaus, which indicates that the cells have reached full confluency (Figure 11). This also suggests that the cells have entered the differentiation program and are beginning to fuse to form myotubes. This is supported by the inverted light microscope images, which depict normal cell growth and shows that as the cells proliferate and become more confluent, differentiation occurs naturally (Figure 12). Recall that differentiation of muscle cells (phenotypically) is indicated by the presence of multinucleated tubes that grow on top of the monocytes. This is seen come Day 6, where the C2C12 cells and pGIPZ scramble control cells fused to form myotubes (Figure 12). This indicates that the C2C12 and pGIPZ cells are terminally differentiated.

The KD1 cells also plateau at Day 5 and have the same growth rate as the control cells (Figure 11). However, there are barely any myotubes seen on Day 6, relative to the controls and the cell count is similar to that of the controls (Figure 11 and 12). On Day 7 the

KD1 cells form myotubes and on Day 8, all three cell lines are fully differentiated. Thus knocking down MLIP results in a delay of C2C12 differentiation.

Figure 11 Knockdown of MLIP protein expression via shRNA does not affect the rate of proliferation Cells were seeded at a low density (~16,000 cells) and were counted daily throughout the course of a week, via the Vi-Cell Cell Viability Analyzer (n=3). ANOVA analysis shows no significant changes within the linear range of the rate of proliferation ($p=0.542$). Note that cells were grown in the absence of puromycin.

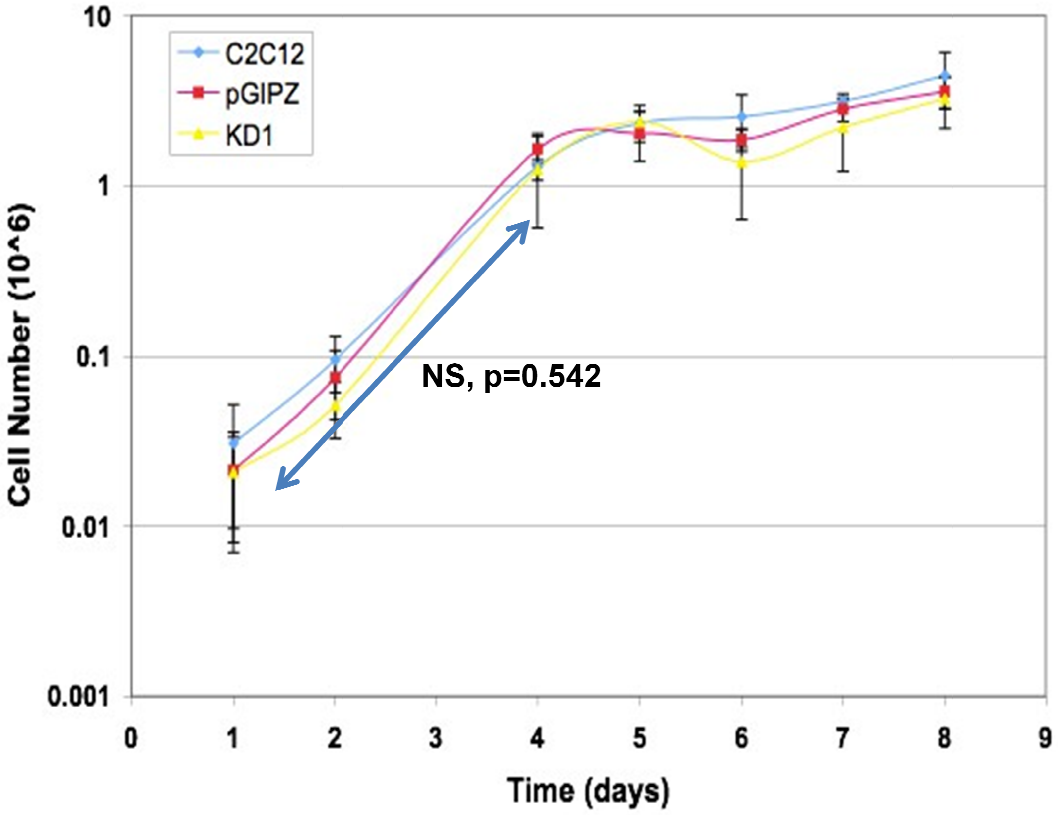
C2C12
pGIPZ
KD1
NS, p=0.542
Cell Number (10^6)
Time (days)
10
1
0.1
0.01
0.001
0
1
2
3
4
5
6
7
8
9

Figure 12 Proliferation of MLIP stably knockdown cell lines Live images were taken using an Olympus CKX41 Inverted light microscope on a daily basis to monitor differentiation as it occurs naturally (n=3). Myotube formation indicates terminal differentiation. Cells were grown in the absence of puromycin.

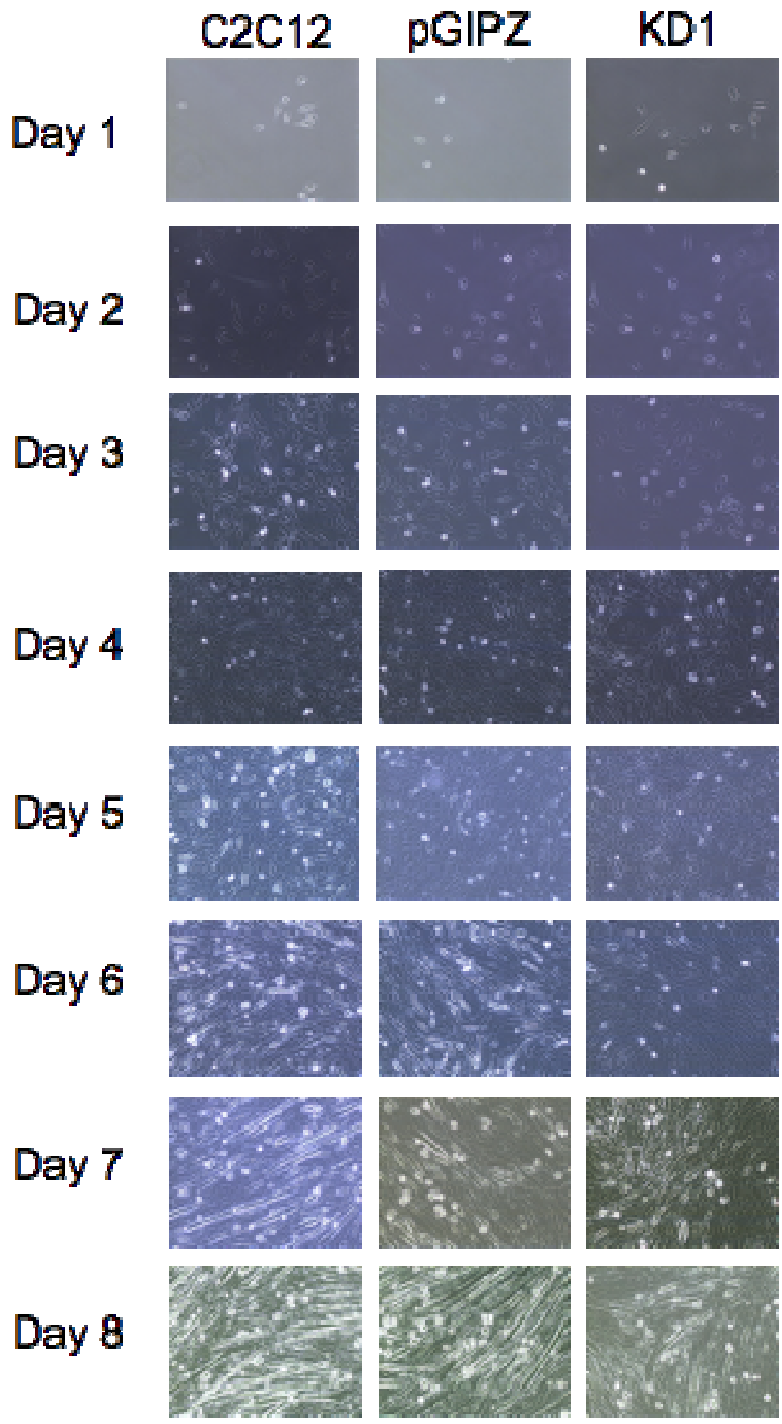
C2C12
pGIPZ
KD1
Day 1
Day 2
Day 3
Day 4
Day 5
Day 6
Day 7
Day 8

3.3 Rescuing the KD1 phenotype by transfection of MLIP

To investigate whether the delay of differentiation seen in the MLIP stably knockdown cells could be rescued, MLIP was re-introduced into the pGIPZ and KD1 cells, by transfecting them with the pcDNA3.1 vector expressing exons 1, 2, 3, 7, 8, 9 of the MLIP gene (pcDNA3.1-MLIP). This vector does not contain the 3'UTR region of the MLIP gene and thus is not targeted by the shRNA lentiviral vectors used to generate the knockdowns. A pcDNA3.1-Control vector was used as the transfection control. Cells were seeded onto 60mm plates and onto gelatin coated cover slips for the purpose of immunofluorescent microscopy. Once the cells reached approximately 60% confluency, they were transfected with pcDNA3.1-MLIP and 24 hours later they were induced to differentiate by withdrawal of serum and replacement with differentiation media (DM) (as previously described). The cells coated onto cover slips were fixed in methanol then stained for the expression of Myosin Heavy Chain (MHC), a marker of terminal differentiation, and with DAPI to identify the nuclei (Figure 13A). Note that the pGIPZ and KD1 cells endogenously express turboGFP (tGFP), since the lentiviral vectors used to make the stable cell lines encodes for this protein. To determine whether or not the delay of myotube formation was rescued by the transfection of pcDNA3.1-MLIP, the fusion index was calculated by counting the total number of myotubes relative to the total number of nuclei (per field of view) (Figure 13B). This is represented in Figure 13B which shows that the KD1 cells have fewer myotubes than the pGIPZ scramble control ($p=0.0233$), after 48 hours of differentiation, regardless of the vector used in the transfection. Transfecting pcDNA3.1-MLIP into the cells did not have a significant impact on the number of myotubes present both before and after differentiation was induced.

Western blots were performed to assess transfection efficiency based on protein expression of pcDNA3.1-MLIP vector, which yields a MLIP isoform with an approximate molecular weight of 35 kDa. The Western blots revealed the presence of this MLIP isoform, suggesting that the transfection was successful; however there was still a decrease in myogenin protein expression (Figure 14). This finding further supports the results seen in Figure 13 where the number of myotubes present in the KD1 cells does not increase post transfection; indicating that the differentiation was not restored. In summary, despite a successful transfection (based on the presence of the expected 35kDa MLIP protein band), there was no change in myogenin protein expression relative to the controls, suggesting that the rescue was not successful in restoring myoblast differentiation.

Figure 13 Analysis of MHC positive cells post transfection with pcDNA3.1-MLIP upon stimulation of differentiation (A) pGIPZ and KD1 cells were grown on to gelatin coated cover slips and transfected with pcDNA3.1-MLIP vector and pcDNA3.1 Control vector to look for a change in the number myosin heavy chain (MHC) positive cells as a reflection of recovery of phenotype. DAPI is stained in blue, MHC is red and tGFP is green (n=3). **(B)** A representation of the fusion index of the KD1 and pGIPZ cell lines post-transfection with pcDNA3.1-MLIP and control vector by identifying the number of MHC positive cells from Figure 14 B relative to the total number of cells per field of view (n=2). Comparison of all transfected groups is statistically significant (ANOVA p=0.061). Comparison of the pGIPZ-Control relative to the KD1-Control shows a decrease in the number of myotubes present post-transfection and differentiation (ANOVA p=0.0233).

A.

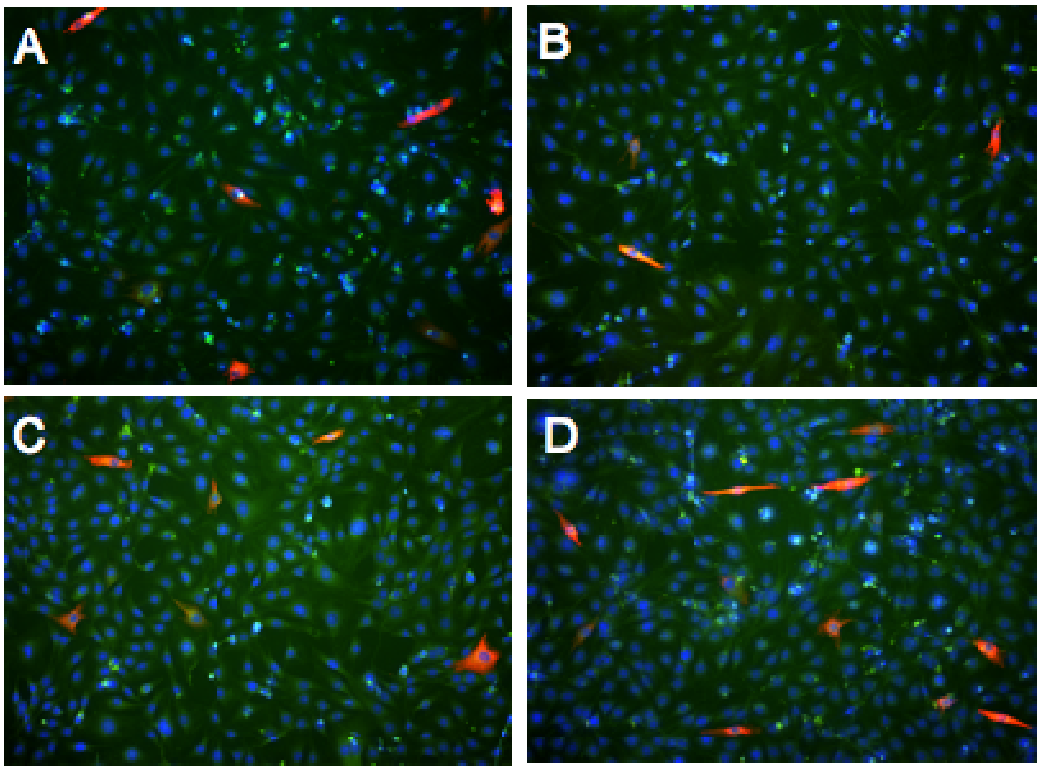
A
B
C
D

B.

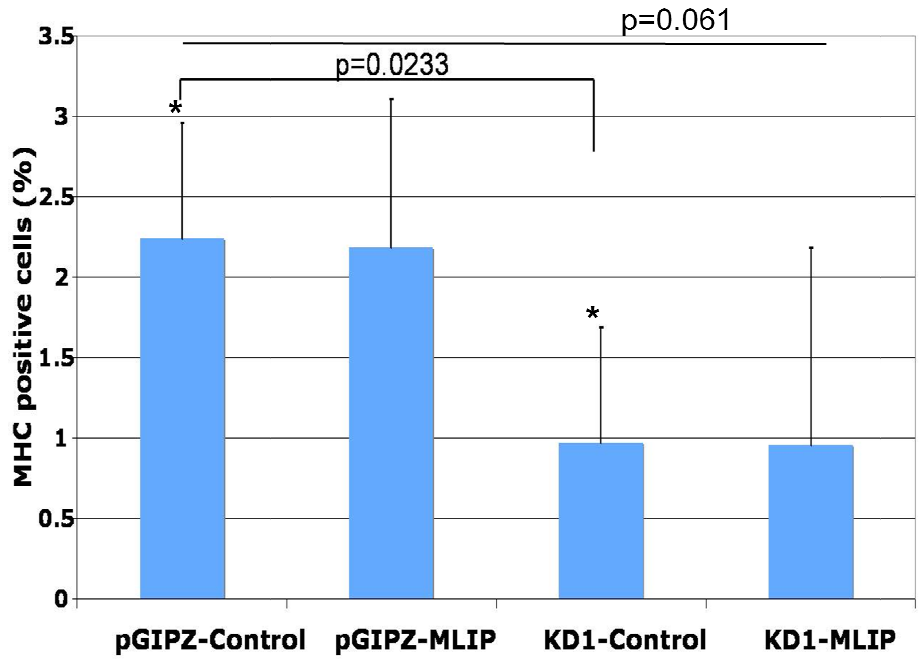
p=0.061
p=0.0233
*
*
MHC positive cells (%)
3.5
3
2.5
2
1.5
1
0.5
0
pGIPZ-Control
pGIPZ-MLIP
KD1-Control
KD1-MLIP

Figure 14 Rescuing the KD1 phenotype by transfection with pcDNA3.1-MLIP (A) MLIP vector and the pcDNA3.1 Control vector was transfected into pGIPZ and KD1 cells then put into DM 24 hours later. Cells were harvested, 24 and 48hrs post differentiation and lysed for Western blot detection. MLIP was examined to see if there was a change in expression. Myogenin was studied to assess whether myotube formation was restored. The transfected MLIP isoform is marked with a red arrow at approximately 35 kDa. Alpha (α)-tubulin was used as the loading control (n=3).

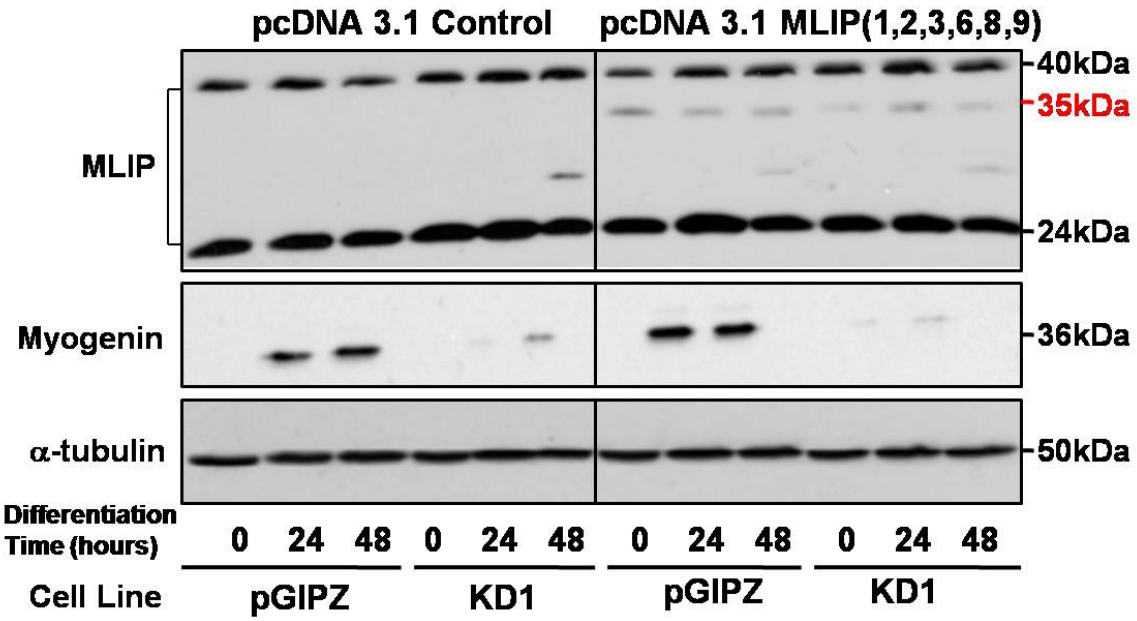
pcDNA 3.1 Control
pcDNA 3.1 MLIP(1,2,3,6,8,9)
MLIP
40kDa
35kDa
24kDa
Myogenin
36kDa
α-tubulin
50kDa
Differentiation Time (hours)
0 24 48 0 24 48 0 24 48 0 24 48
Cell Line
pGIPZ
KD1
pGIPZ
KD1

3.4 Down regulation of MLIP protein expression does not alter LMNA protein expression

Since MLIP was discovered through its interaction with lamin A/C, we asked if the knockdown of MLIP affects lamin A/C protein expression. To do this, C2C12, pGIPZ and KD1 cells were seeded onto 60mm plates and grown to 60% confluency. Then, the cells where induced to differentiate by withdrawal of serum and replacement with (DM). For the course of 5 days, the cells were kept in DM and subsequently harvested at 0, 24, 48, 72, 96, 120 hours post differentiation. The cells were lysed and the lysates were quantified for total protein via Bradford quantification. The cell lysates were then analyzed through immunoblotting where MLIP, lamin A/C, and α-tubulin were examined (n=3) (Figure 15). Figure 15 shows that both lamin A and C protein expression is relatively the same between the control cells and the KD1 cells. This was done repeatedly and no visible change in lamin A/C protein expression was seen. Thus, the knockdown of MLIP does not affect the protein expression of lamin A/C in C2C12 cells.

Further analysis of Figure 15 shows that MLIP protein expression in the KD1 cells have returned to normal levels relative to pGIPZ and C2C12 cells. This was unexpected because the knockdown cell lines were generated under puromycin selection and were previously genotyped to ensure the presence of the shRNA constructs. The difference between the original observations and this result is that the cells were no longer grown under puromycin selection. Puromycin is the selection reagent used in generating the stable cell lines. This experiment was done repeatedly in the absence of puromycin. In fact, the original immunofluorescent images of the knockdown cells established by Ahmady were also done in the presence of puromycin. All of the experiments, post Ahmady's work, were done in the

absence of puromycin and still a delay in C2C12 myoblast differentiation was seen in the KD1 cells in contrast to the controls (Figure 12). Perhaps the presence of puromycin affects the protein expression of MLIP in the KD1 cells.

Figure 15: Stably knockdown MLIP protein expression does not affect LMNA expression C2C12, pGIPZ, and KD1 cell lines were grown to confluency then forced to differentiate throughout the course of 5 days by withdrawal of serum. Cells were lysed for Western blot detection probing for MLIP, LMNA, and α-tubulin (n=4).

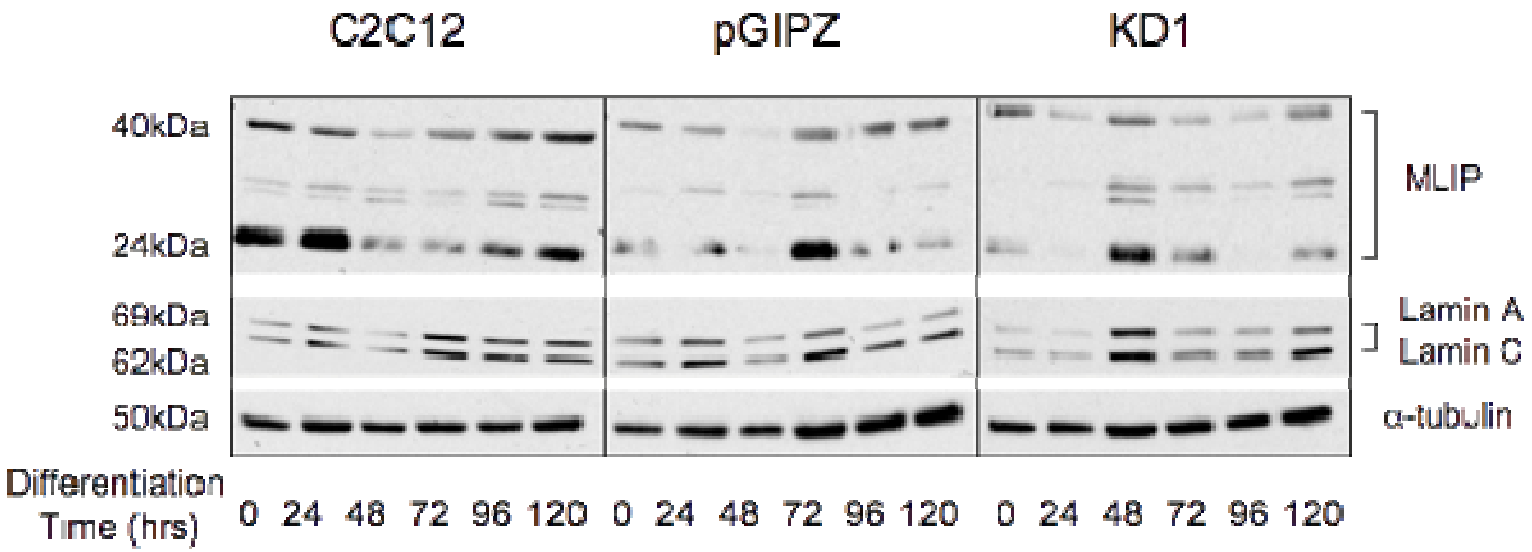
C2C12
pGIPZ
KD1
40kDa
24kDa
69kDa
62kDa
50kDa
MLIP
Lamin A
Lamin C
α-tubulin
Differentiation Time (hrs)
0 24 48 72 96 120 0 24 48 72 96 120 0 24 48 72 96 120

3.5 The presence of Puromycin affects MLIP protein expression

To determine if puromycin has an effect on MLIP expression in the stable cell lines, pGIPZ, KD1, and KD3 cell lines were cultured in the presence or absence of puromycin (Figure 16). Since KD3 was part of the original studies established by E. Ahmady, it was re-introduced into these experiments for the purposes of reproducing Ahmady's original work. The stable cell lines were grown in the presence of 1.5µg/ml of puromycin (with the exception of wild type C2C12 cells which were not treated with puromycin), until they reached confluency. The cells were then seeded onto 60mm plates where one set was kept under selection and the other set was removed from selection for a period of 24 hours. The cells were harvested and lysed for Western blot detection (Figure 16). Note that the wild type C2C12 cells were not treated with puromycin in order to show the normal MLIP expression pattern. In Figure 16 the red box highlights the cells that were treated with puromycin, which were the pGIPZ, KD1 and KD3 cells. Both knockdown cell lines show a decrease in MLIP expression relative to the treated pGIPZ control, however only in the presence of puromycin. This affect is lost once puromycin is removed for a period of 24 hours. Therefore, puromycin affects MLIP protein expression in normal C2C12 cells and the knocked down cell lines.

Figure 16 Treatment with puromycin affects MLIP protein expression C2C12, pGIPZ, KD1 and KD3 cells were grown to confluency with or without the presence of 1.5 μg/mL puromycin (over a period of 24 ours), where only pGIPZ, KD1, and KD3 were treated with puromycin. Note that the cells treated in puromycin are highlighted in a red box, which does not include C2C12 cells. This was to provide a direct comparison to MLIP expression in C2C12 cells. Cells were then lysed for Western blot detection, examining MLIP and α-tubulin (n=2).

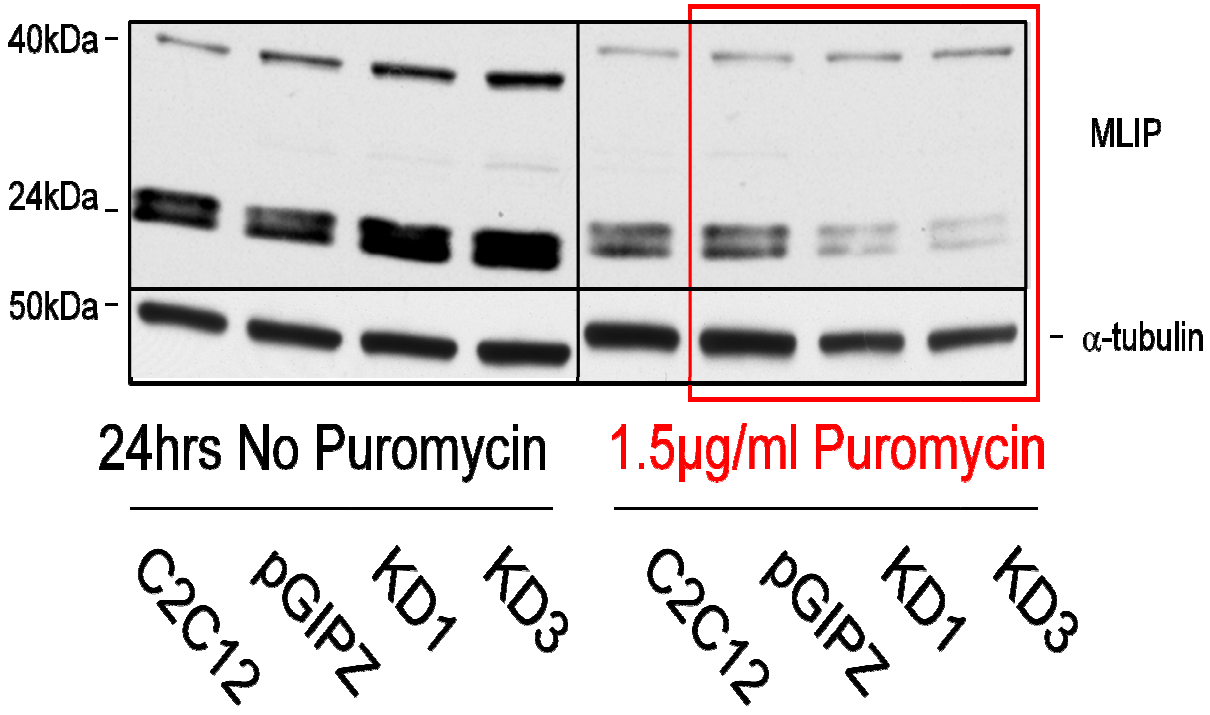
40kDa
24kDa
50kDa
MLIP
α-tubulin
24hrs No Puromycin
1.5µg/ml Puromycin
C2C12
pGIPZ
KD1
KD3
C2C12
pGIPZ
KD1
KD3

3.6 Generating new MLIP stably knocked down C2C12 cells

Given the affects of puromycin on the pGIPZ, KD1 and KD3 cells, new knockdowns were generated using the same lenti viral vectors and the same transfection approach, with the exception that single colonies were not selected thus leaving a mix of colonies. The vectors were transfected into 50% confluent C2C12 cells using Lipofectamine 2000 reagent where 48 hours post transfection, the cells were put under selection using 1.5μg/ml of puromycin for 3 weeks. Every two days the growth media containing puromycin was replenished. Rather than selecting single colonies (as did Ahmady in generating the stable cell lines) a polyclonal approach was used where all of the colonies were allowed to proliferate (ie. Using batch culture). The advantage of this method is that it is less time consuming than isolating and purifying colonies. Thus, generating a new scramble control cell line called pGIPZ-A, and two new knockdown cell lines (using the KD1 and KD3 vectors) were referred to as KD1-A and KD3-A (respectively) (Figure 17).

Immunoblotting of all three new cell lines was performed to examine MLIP protein expression (Figure 17). It is shown that the new KD1-A and KD3-A cell lines have less MLIP protein expression relative to both the pGIPZ-A scramble controls; primarily of the 22 and 24kDa protein bands (Figure 17). Furthermore, Lamin A and C protein levels remained unaffected by the MLIP knockdown as previously shown. Prior experiments suggest that under selection, the loading control, α-tubulin, is affected by puromycin and thus the exact same amount of total protein lysates were loaded onto SDS-PAGE gels for Coomassie Blue staining, in addition to immunoblotting (Figure 17B). The boxes in red highlight prominent bands that show equal loading of total protein. The KD1-A column has a unique band that stands out, which may be a reflection of shRNA specifically used to generate the KD1-A

MLIP knockdown. Thus, under the presence of puromycin, MLIP is stably knocked down in C2C12 cells.

3.6.1. The affects of puromycin on the new MLIP stably knocked down C2C12 cells

To determine if puromycin has an effect on the new knockdowns, they were seeded on 60mm plates without puromycin for a period of 24 hours. Following this, the cells were lysed and analysed via Western blot (Figure 18). Upon removal of puromycin, MLIP protein expression returned to normal levels relative to the controls. This was previously seen in the KD1 and KD3 cell lines. In conclusion, puromycin affects MLIP protein expression despite the presence of the PuroR resistance gene that is incorporated into the C2C12 cell genome.

Figure 17 A new MLIP stably knockdown cell line (A) C2C12 cells were transfected with pGIPZ backbone based shRNA lenti vectors, and were then selective for resistance against puromycin, for a period of three weeks. Cells were lysed to determine if a knock down of MLIP protein levels was achieved. Both MLIP and lamin A/C were examined where α-tubulin was used as a loading control. (B) 10μg of total protein lysate were loaded on to SDS-PAGE gels, run following standard procedures than stained with Coomassie Blue to show equal loading between lanes. The red boxes identify bands that are equally loaded.

A.

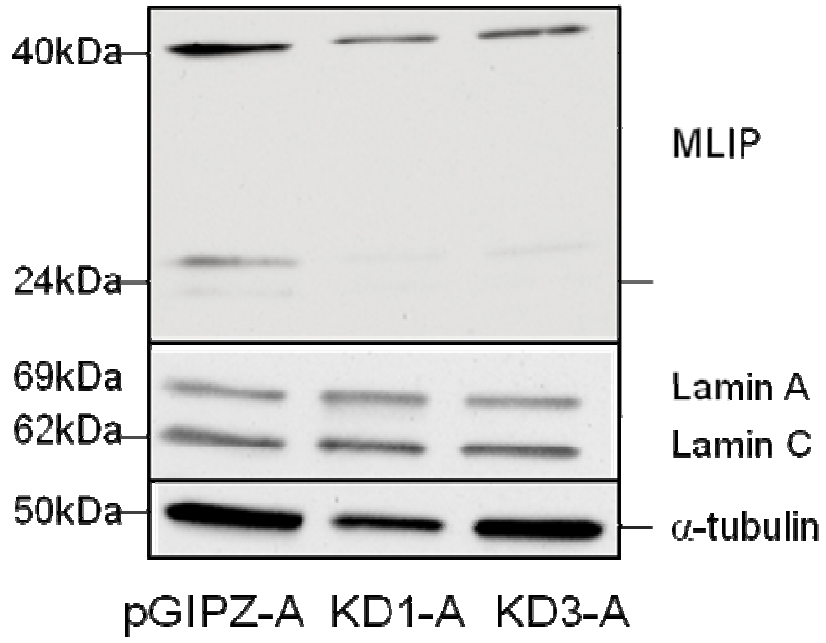
40kDa
24kDa
69kDa
62kDa
50kDa
MLIP
Lamin A
Lamin C
α-tubulin
pGIPZ-A KD1-A KD3-A

B.

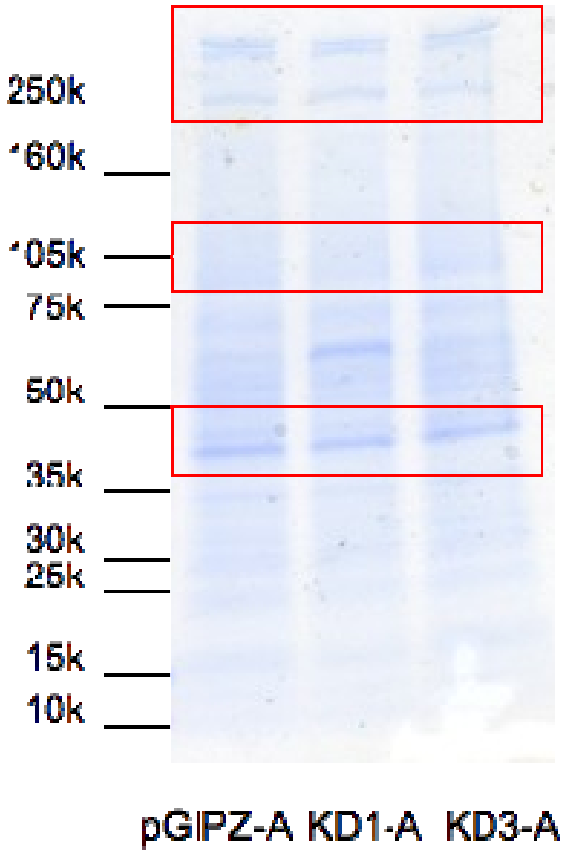
250k
160k
105k
75k
50k
35k
30k
26k
15k
10k
pGIPZ-A KD1-A KD3-A

Figure 18 The removal of puromycin restores MLIP protein expression levels in MLIP stably knocked down C2C12 cells. PGIPZ-A, KD1-A, and KD3-A cells were cultured in 60mm plates without puromycin for a period of 24hours. Cells were lysed and analyzed via immunoblotting. MLIP and lamin A/C protein levels were examined for changes in expression. α-tubulin was the loading control (n=3).

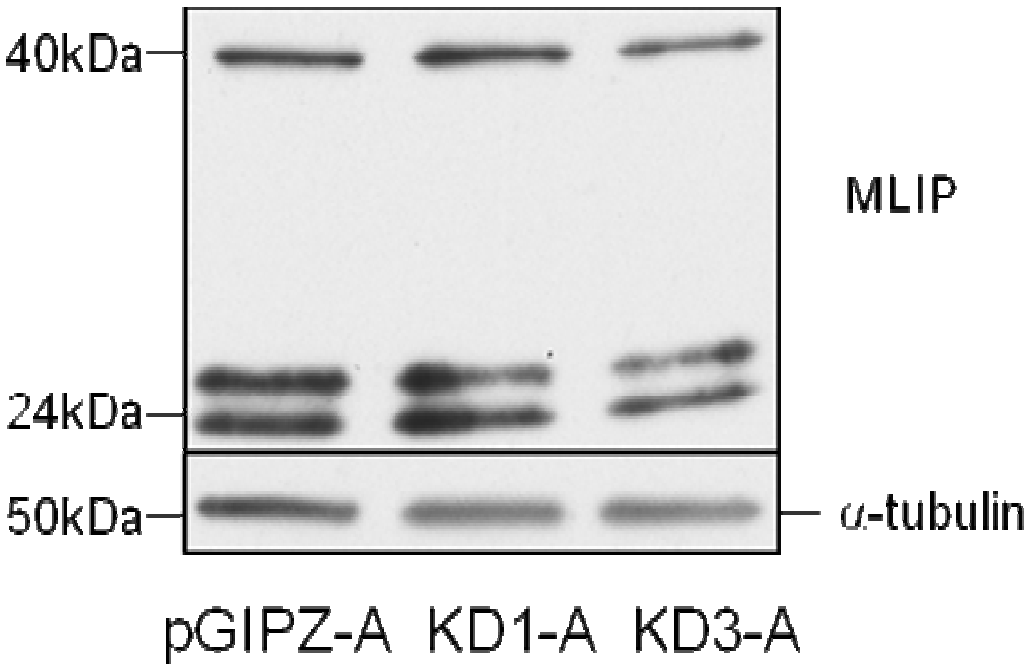
40kDa
24kDa
50kDa
MLIP
α-tubulin
pGIPZ-A KD1-A KD3-A

Chapter 4: Discussion

Discussion

A-type lamins are associated with a multitude of diseases including EDMD, LGMD, CMT, and partial lipodystrophy, all of which target various tissues in the body. Though A-type lamins are not the only cause of myopathies, their involvement in disease is very intriguing given that some mutations of LMNA are tissue restricted and others are not. Understanding the mechanism of laminopathies lead us to the discovery of a novel Muscle-enriched A-type lamin-interacting protein referred to as MLIP. MLIP is enriched in brain, heart and skeletal tissue (Figure 3), which conquer with MLIP expression profile of normal mouse tissues as reported by published data shared on GEO profiles (Supplementary Figure S6; Thorrez *et al*, 2008). Preliminary data, using transient *LMNA* knockdowns in C2C12 cells demonstrated that MLIP protein levels increase upon knocking down LMNA, primarily upon knocking down lamin A (Supplementary Figure S1). The focus of this work was to explicate the biological role of MLIP in myogenesis using the MLIP stably knocked down C2C12 cell line, generated by a former student of the laboratory.

The global gene effect of knocking down MLIP was studied through exon microarrays, using extracted RNA from the KD1 cell line and accompanying controls, in the absence of puromycin (the selective reagent). Initially, our interests were in differentially regulated transcription factors (TFs) and a set of TFs was used to validate the arrays (Table 4; Figure 7). However, it soon became clear that gene expression is different between normal C2C12 cells and the pGIPZ scramble control cells. For example, the KD1 cells compared to the pGIPZ cells show a 5-fold increase in Pax7 expression (Figure 8). This would suggest that the KD1 cells are dedifferentiating into satellite cells since, only satellite cells express Pax7 (Olguin and Olwin, 2004). This could potentially explain why a delay of

muscle differentiation is seen upon withdrawal of growth media (Figures 11 and 12). However, comparison of KD1 to C2C12 cells shows a 70% reduction Pax7 gene expression (Figure 8). This discrepancy may be a reflection of the fact that the random integration of the pGIPZ lenti viral vector cannot be controlled and where it integrates may have an impact on gene function and/or cell function at large. Though, no noticeable phenotypic changes where observed in the pGIPZ cells, it is possible that different pathways were affected by generating the pGIPZ stable cell line. For these reasons, a new approach was used to study the arrays.

A venn diagram was generated to search for genes uniquely regulated in only the KD1 versus pGIPZ ANOVA analysis (Figure 9). This yielded 166 differentially regulated genes that were uploaded into DAVID, an online database sponsored by the NIH, looking for any diseases related to these genes (Table 5). Thirty of the 166 genes are associated with diseases or disease phenotypes (Table S2). Five of the disease associated genes include: *DMPK, HSPB8, LMNB2, NEFL*, and *SGCD*. Mutations of these genes are directly linked to laminopathies, myopathies, and neuropathies, paralleling that which is seen in LMNA mutations (Table 6).

LMNB2 (which encodes for lamin B2) is down-regulated in the microarrays; mutations of *LMNB2* cause Acquired partial lipodystrophy (APL) (Padiath *et al*, 2006; Hegele *et al*, 2006). This causes the loss of subcutaneous fat in the upper body and accumulation in the lower body. Thus far, it is the only known laminopathy linked to *LMNB2* (Padiath *et al*, 2006; Hegele *et al*, 2006). Though MLIP was discovered through its involvement with lamin A/C, B-type lamins are expressed throughout development of all cells (D'Angelo and Hetzer, 2006; Vergnes *et al*, 2004). Perhaps, MLIP and *LMNB2* interact

early on in development and are more linked to one another than originally thought. This remains to be elucidated.

Diseases of striated muscle, in particular, cardiomyopathies and muscular dystrophies, share a similar pathology where there is a loss of muscle (Heydemann *et al*, 2006). Perhaps MLIP plays a role in the overlap seen within these pathologies. Fascinatingly, gene expression profiles of septal myocardial tissue samples from patients with DCM have elevated MLIP expression levels compared to patients with non-failing hearts (Supplementary Figure S5; Barth *et al*, 2006). Furthermore, gene expression profiles using quadriceps muscle tissue from patients with Duchenne Muscular Dystrophy, exhibit decreased MLIP expression levels relative to normal individuals (Supplemental Figure S3; Haslett *et al*, 2003). Mutations of the dystrophin-glycoprotein complex can cause different forms of muscular dystrophies and DCM (Crosbie *et al*, 1999; Tsubata *et al*, 2000). In particular, S151A mutation of *SGCD* (which encodes for the δ-sarcoglycan, a 35 kDa dystrophin-associated glycoprotein) causes DCM1L (Tsubata *et al*, 2000) and a single nucleotide deletion of 656C in exon 7 of *SGCD* gene changes the reading frame and causes LGMD2F (Nigro *et al*, 1996). In addition, gene expression profiles of patients with LGMD2A express lower MLIP transcript levels relative to non-affected controls (Supplemental Figure S4).

Dystrophia myotonica 1 (DM1, or myotonic dystrophy 1) is a multi-systemic disease where patients exhibit muscle wasting and cardiomyopathy (McNally and Pytel, 2007). The disease itself is a result of a "trinucleotide expansion of CTG in the 3'UTR region of the myotonic dystrophy protein kinase" (*DMPK*) gene (Brooke *et al*, 1999; Harmon *et al*, 2008). Other studies show that DM1 patients also have decreased DMPK expression (Harmon *et al*,

2008). Similarly, decreasing MLIP protein expression also causes a decrease in *DMPK* mRNA levels. What's more, ChIP-on-CHIP analysis of MLIP identified *DMPK* as a transcriptional target (Supplementary Figure S2). *DMPK* is expressed in embryonic myocytes (Harmon *et al*, 2008), as is MLIP, and *DMPK* is needed for muscle differentiation (Harmon *et al*, 2008). Taken together, perhaps MLIP is involved in *DMPK* regulation and may be affected by the pathogenesis of DM1. Thus, it appears that MLIP may also be involved in the striated muscle-associated diseases.

It is well established that A-type laminopathies also cause various neuropathies including CMT. Upon down-regulating MLIP expression, an almost 2-fold increase in NEFL transcript levels and an approximate 2-fold decrease in *HSPB8* transcript levels is seen. Mutations of *NEFL* (neurofilament, light polypeptide) and *HSPB8* (heat shock (22kDa) protein 8) cause CMT, where mutations of *NEFL* result in CMT1F and CMT2E (Ismailov *et* al, 2001; De Jonghe *et al*, 2001) and *HSPB8* cause CMT2L (Tang *et al*, 2005). Furthermore, mutations of *HSPB8* also cause distal hereditary motor neuropathy (type II), a neuropathy causing muscle atrophy of the toes and feet (Irobi *et al*, 2004). CMT1 is a demyelination neuropathy whereas CMT2 is an axonal neuropathy that mostly affects the lower body, however both affect nerve signal conduction, eventually leading to muscle wasting (Berger *et al*, 2002). Thus far, no known lipodystrophy or neuropathy profiling studies of MLIP are available. Further analysis of the microarray data using DAVID, shows that *NEFL* is involved in several biological processes including neuron projection regeneration, axon regeneration, and regulation of neuron differentiation (Table S1). MLIP may have a role in neurogenesis and affect proteins implicated in neuropathies.

DAVID analysis also revealed the involvement of *EYA1* in the regulation of neuronal differentiation (Table S1). Previous work using ChIP-on-CHIP analysis of MLIP also identified *EYA1* and *SIX5* as potential regulatory target (data not shown). *SIX5* and *EYA1* are involved in early development of myogenesis and more specifically during embryogenesis. They are involved in early activation of MRFs and later on during differentiation (Fougerousse *et al*, 2002). Both Eya1 and Six5 are highly expressed in adult skeletal muscle (Spitz *et al*, 1998; Abdelhak *et al*, 1997; Fourgerousse *et al*, 2002) Six5 is found downstream of *DMPK* (Winchester *et al*, 1999) and is implicated in myotonic dystrophy (Klesert al, 2000; Sarkar *et al*, 2000). In fact, the CTG triple repeat found within the 3'UTR region of *DMPK* gene, is also within the promoter region of *SIX5* gene (Boucher *et al,* 1995; Winchester *et* al, 1999). The unstable expansion of the CTG repeat suppresses *SIX5* expression (Klesert *et al*, 1997). Collectively, this evidence further supports MLIP's involvement in muscle development.

Future studies will include validating the transcriptional changes of *DMPK*, *HSPB8*, *LMNB2*, *NEFL*, and *SGCD* as seen in the exon microarrays. One could argue that these fold changes are small, despite the fact that they are statistically significant. However, examination of mRNA levels does not always parallel the resultant protein levels. Possible reasons for this may be a result of recycling of mRNA transcripts, that could potentially increase the protein yield, or the mRNA transcripts could be targeted in such a manner that would prevent protein translation (ie. The miRNA pathways). Future work examining both the transcriptional and translational impact of the *DMPK*, *HSPB8*, *LMNB2*, *NEFL*, and *SGCD* on MLIP will clarify their role in muscle development.

The second part of this project was to characterize the role of MLIP during proliferation and differentiation by using the MLIP stably knockdown cell line. To do this, a simple proliferation study was employed to see if there was a difference in growth rates comparing the KD1 cells to the normal C2C12 cells and the pGIPZ cells, in the absence of puromycin (Figures 11 and 12). There was no difference in growth rate but the KD1 cells did take longer to differentiate and thus knocking down MLIP resulted in a delay of differentiation.

Attempts to rescue the phenotype were not successful. Though the transfections worked, based on the detection of the expected MLIP protein band, there was no difference in the number of myotubes when comparing KD1 to pGIPZ cells that were transfected with either the pcDNA3.1-Control vector or the pcDNA3.1-MLIP vector (Figure 14). This may be a reflection of the fact that C2C12 cells are known to have a low transfection efficiency using cationic lipids, such as Fugene6 and Lipofectamine2000 transfection reagents, and so these means of transfection are not strong enough to induce a rescue of phenotype. Luciferase assays comparing gene expression of different nonviral gene transfer reagents in different cell lines, demonstrated that using Lipofectamine2000 in C2C12 cells generated the lowest gene expression compared to other reagents (Yamano *et al*, 2010). Another study looked at transfection efficiency based upon fluorescent measurements and demonstrated that transfections using Fugene6 and Lipofectamine2000 yielded similar results (Susa *et al*, 2008). Taken together, this would suggest that FuGENE6 based transfections in C2C12 cells are not capable of rescuing the MLIP knocked down phenotype. Aside from the transfection efficiencies, it is possible that the vector itself was missing key exons responsible for MLIP protein expression. The vector used for the transfections was designed by another student

studying the different MLIP isoforms and found that exons 1, 2, 3, 7, 8, 9 were present in most isoforms (all exons, except exon 2, were found in most isoforms) and so it seemed reasonable to use it for the recovery experiments. Future studies would include generating a stable cell line via retroviruses, which is the best method to ensure successful infection and incorporation of the viral vector into the cell's genome.

Given that preliminary data demonstrates that knocking down *LMNA* increase MLIP expression, we looked to see if knocking down MLIP would also affect lamin A/C protein expression (Supplementary Figure S1). Western blots show that lamin A/C was not affected by knocking down MLIP (Figure 15). In spite of this, it became clear that throughout the course of these experiments MLIP expression had returned to normal protein levels, relative to the C2C12 wild type cells (Figure 15). However, the delay in differentiation was still present as depicted by the graphical representation of the number of myotubes seen upon stimulation of differentiation in the recovery experiments (Figures 13) and in the representative Western blots indicating a decrease in myogenin protein levels, a marker of differentiation (Figure 14). These cells were no longer kept under puromycin selection and so it was initially thought that the cells where losing pGIPZ backbone expression vector, yielding non-transfected cells. Puromycin is an aminonucleoside antibiotic produced by *Streptomyces alboniger*, which blocks protein synthesis (Yarmolinsky and De La Haba, 1959). It does so by preventing the peptidyl transfer on ribosomes (Vazquez 1979; de la Luna and Ortin, 1992). Therefore, without the puromycin N-acetyl-transferase (PAC) resistance gene, cells will die due to apoptosis (de la Luna and Ortin, 1992). This gene is encoded into the pGIPZ backbone vector (ie. PuroR marker, refer to OpenBiosystems

manual). To confer resistance to puromycin, the stable cells were studied under puromycin selection, to see if MLIP expression would decrease as previously shown (Figure 16).

Figure 16 demonstrates that treatment with puromycin does in fact knockdown MLIP protein levels. The stable cell lines were grown to confluency in the presence of puromycin and were seeded onto 60 mm plates. Once the cells were 50 % confluent, puromycin was removed from one group of cells, for a period of 24 hours. The cells were lysed and quantified using the Western blot approach. The red box in Figure 16 identifies the cells that were treated with puromycin. C2C12 cells were not treated with puromycin because it would induce cell death since the wild type cells lack the puromycin resistance gene (PAC). Notice that only the cells kept under selection, exhibit a decrease in MLIP expression relative to the pGIPZ controls (Figure 16). The KD3 cells also depict a decrease in MLIP protein expression, primarily of the 24kDa molecular weight band (Figure 16). It is important to note that under selection, the stable cells take longer to proliferate and take more time to trypsinize relative to cells not under selection (data unreported). Furthermore, despite quantifying total protein to ensure that equal loading of protein lysates was performed, all of the puromycin treated cells had variations in protein expression of the α-tubulin (Figures 16). This was not seen in the untreated groups, which is why α-tubulin was still used as the loading control for the experiments. Since puromycin prevents protein translation, there could be a delay in protein production that varies between the stable cell lines in view of the fact that each cell line originated from a unique single colony. The shRNA integration site is different in each cell line and thus the location of the integration site may impact protein expression. We know that the vectors are being expressed since the stables express tGFP, thereby indicating successful vector integration into the genome

(Figure 13). To investigate this further, new stable cell lines were generated (Figure 17). Once again, when puromycin was removed the knockdown affect was lost. Taken together, this result suggests that MLIP and puromycin somehow interact and that perhaps a "conditional knocked down cell line" was generated instead.

Our lab has demonstrated that MLIP co-localizes with PML bodies within the nucleus of the cell. PML bodies consist of PML protein, SUMO and more than 50 proteins that are localized or transiently found within them (Moran *et al*, 2009). PML bodies have been associated with many regulatory functions including DNA repair, apoptosis, proteasomal degradation and gene repair, but the exact function of PML bodies is elusive (Moran *et al*, 2009). Wang *et al*., demonstrated that PML is not needed for survival but is essential for several apoptotic pathways (Wang *et al*, 1998). A study by Moran *et al*.; demonstrated that cell lines transfected with vectors expressing the PAC (puromycin resistance) gene causes re-localization of PML bodies (Moran *et al*, 2009). This effect was seen in several different vectors (both scramble control and empty vector controls). Vectors that express the PAC gene caused clustering/aggregation of PML within the nuclei. They also found that HSP70, SUMO-1, and 20S proteasome were aggregating and were co-aggregating with PML or were localizing around PML. Some aggregates were seen localizing within the cytoplasm. They concluded that the PAC gene is needed for PML and HSP70 co-agregatoin. These effects were not seen with vectors expressing other selection markers. Lastly, they demonstrated that stable cells generated via puromycin selection no longer displayed PML aggregates. The authours point out that the presence of the PAC gene may have an impact on other proteins and should be taken into account upon designing experiments. This can potentially explain the puromycin affect seen on MLIP expression

within the KD1 and pGIPZ cells. It may be linked to the conditional knockdown of MLIP that is seen with puromycin treatment. This would also suggest that shRNA vectors containing the puromycin gene are not suitable for generating MLIP knockdowns and so future studies would be to generate a stable cell line using a shRNA vector that contain other selective markers. It also emphasizes that MLIP may have a bigger role in PML bodies than originally thought.

A study looking at the therapeutic benefits of puromycin found that it formed complexes with melanin in fibroblast cells (Wrzesniok *et al*, 2005). Another group found that melatonin promoted puromycin-induced apoptosis within HL-60 cells, an acute promyelocytic leukemia cell line (Koh *et al*, 2011). Collectively, this body of evidence shows that puromycin is not just an antibiotic or a selection reagent and further supports the argument that MLIP and puromycin somehow interact. Puromycin induces cell death via apoptosis and PML bodies have been associated with apoptosis, so it's very possible that MLIP is also involved in the apoptotic pathway.

Although our attempts at generating an *in vitro* stably knocked down cell line was not truly successful, an *in vivo* heterozygous MLIP knockdown mouse model (Cre-CMV; $MLIP^{+/-}$) was generated (Supplementary Figure S7). Preliminary data suggests that upon removal of one *MLIP* allele, MLIP protein expression of mouse hearts and skeletal tissue is drastically decreased relative to the wild type controls (Supplemenatry Figure S8). Lamin A/C protein expression was not affected. The level of protein reduction was not expected. The mice are viable, however, to date, no homozygous null MLIP mouse has been observed. Therefore a complete loss of MLIP may be embryonically lethal in the mouse. Future studies using this mouse model will elucidate the biological/developmental role of MLIP.

In summary, the data presented herewith suggests that MLIP is not essential for C2C12 mouse myoblast differentiation but may be involved in the process. The work on the Cre-CMV; $MLIP^{+/-}$ mouse model is early days and future experiments will provide insight into MLIP's involvement in myogenesis and potentially other biological processes such as neurogenesis. The microarray data highlights possible links to different muscle wasting diseases, neuropathies and lipodystrophies. MLIP clearly interacts with puromycin. The knockdown studies demonstrate that MLIP is conditionally knocked down upon treatment with puromycin. Nonetheless, with or without the presence of puromycin, we see a delay in differentiation (Figures 11-14). These findings impact the results of the microarrays, given that the knocked down cells used in the microarray experiments were cultured without puromycin, which in turn restored MLIP protein levels. The goal of this endeavour was to look for novel pathway interactions without the presence of MLIP, which brings into to question the overall interpretation of the results. Data that is highlighted is supported by work done previously in lab. ChIP-on-CHIP data confers with the exon microarray data to show that MLIP is associated with transcription factors and regulatory binding elements that are involved in myogenesis. This may shed light upon the development of disorders such as dystrophia myotonica 1 and other neurodegenerative diseases. Currently, very little is known about MLIP function and future studies involving the Cre-CMV; $MLIP^{+/-}$ mouse model will help to explicate the biological function of MLIP and whether or not it has a role in the pathogenesis of muscle-related disorders.

Appendix

Figure S1 Transient knockdowns of *LMNA* in C2C12 cells C2C12 cells were transfected with *LMNA* pGIPZ based, shRNA lenti vectors to knockdown lamin A/C protein expression. MLIP expression was analyzed and GAPDH was used as the loading control.

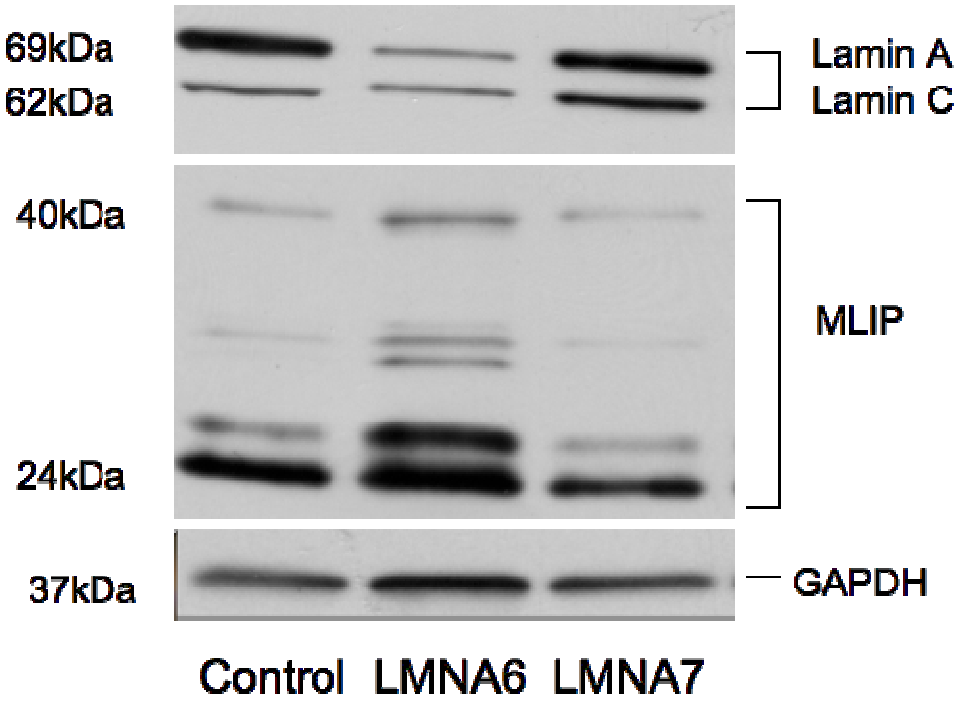
69kDa
62kDa
Lamin A
Lamin C
40kDa
MLIP
24kDa
37kDa
GAPDH
Control
LMNA6
LMNA7

Table S1: Selected biological processes as determined by DAVID analysis using the differentially regulated genes affected in knocking down MLIP expression

Neuron projection regeneration			
BCL2	NEFL		
Axon regeneration			
BCL2	NEFL		
Regulation of neuron differentiation			
BCL2	NEFL	EYA1	YWHAG

Table S2 Differentially regulated genes and associated diseases

Gene	Protein Name	Associated Disease/Phenotype
Abo	ABO blood group	Inflammatory adhesion response Influence plasma levels of liver enzymes
Bcl2	B-cell CLL/lymphoma 2	Leukemia/lymphoma, B-cell, 2,
Jak2	Janus Kinase 2	Budd-Chiari syndrome Crohn's disease Acute Myelogenous Leukemia Myeloproliferative disorders
Marveld2	MARVEL domain containing 2	Deafness, autosomal recessive 49
Sh2d1a	SH2 domain protein 1A	Lymphoproliferative syndrome (X-linked)
Aim1	Absent in melanoma 1	Ischaemic stroke
Adarb1	Adenosind deaminase RNA-specific, B1	Pulmonary function measures
Ano5	Anoctamin 5	Gnthodiaphyseal dysplasia,
Bmpr1b	Bone Morphogenetic prtein receptor, type IB	Brachydactyly type A2 Chondrodysplasia
Capn10	Calpain 10	Diabetes mellitus type 1
Ccr5	Chemokine (C-C motif) receptor 5	Diabetes mellitus type 2 Resistance to Hepatitis C virus Susceptibility/resistance to HIV infection Susceptibitily West nile virus
Cc2d1a	Coiled-coil and C2 domain containing 1A	Mental retardation, autosomal recessive 3
Dmpk	**Dystrophia Myotonica-protein kinase**	**Dystrophia myotonica 1**
Eya1	Eyes absent homolog 1	Anterior segment anomalies and cataract Branchiootic syndrome Branchiootorenal syndrome Melnick-Fraser syndrome Otofaciocervical syndrome
Hspb8	**Heat shock 22kDa protein 8**	**Charcot-Marie-Tooth disease type 2L Distal hereditary motor neuropathy type II**
Hmga2	High mobility group AT-hook 2	Adult and childhood (stature) Lipoma and Lipomatosis Salivary adenoma Uterine leiomyoma
Hnmt	Histamin N-methyltransferase	Asthma
Hcrt	Hypocretin (orexin) neuropeptide precursor	Narcolepsy 1
Il1rl1	Interleukin 1 receptor-like 1	Celiac disease

		Immune response
Il10	Interleukin 10	Graft-versus-host disease Protection against HIV-1 Rheumatoid arthritis Ulcerative colitis
Lmnb2	**Lamin B2**	**Acquired partial Lipodystrophy**
Lrrc16a	Leucine rich repeat containing 16A	Serum-transferrin levels
Mmab	Methylmalonic aciduria cblB type	Dyslipidemia Methylmalonic aciduria
Nefl	**Neurofilament, light peptide**	**Charcot-Marie-Tooth disease (type 1F)** **Charcot-Marie-Tooth disease (type 2E)**
Pkp1	Plakiphilin 1	Ectodermal dysplasia/skin fragility syndrome
Pp2r2b	Protein phosphatase 2, regulatory subunit B, beta isoform	Spinocerebellar ataxia 12
Sgcd	**Sarcoglycan, delta**	**Cardiomyopathy, dilated (1L)** **Multiple sclerosis** **Limb-girdle Muscular dystrophy (2F)**
Thbd	Thrombomodulin	Myocardial infarction Thrombophilia
Xpc	Xeroderma pigmentosum, complementation group C	Xeroderma pigmentosum, group C,
Zfat	Zinc finger AT hook domain containing	Autoimmune thyroid disease 3

Note: Bolded genes are highlighted in Table 6 of Results.

Figure S2 A comparison of the ChIP-on-CHIP data versus the Exon Microarrays
ChIP-on-CHIP analysis was performed by E.Ahmady.

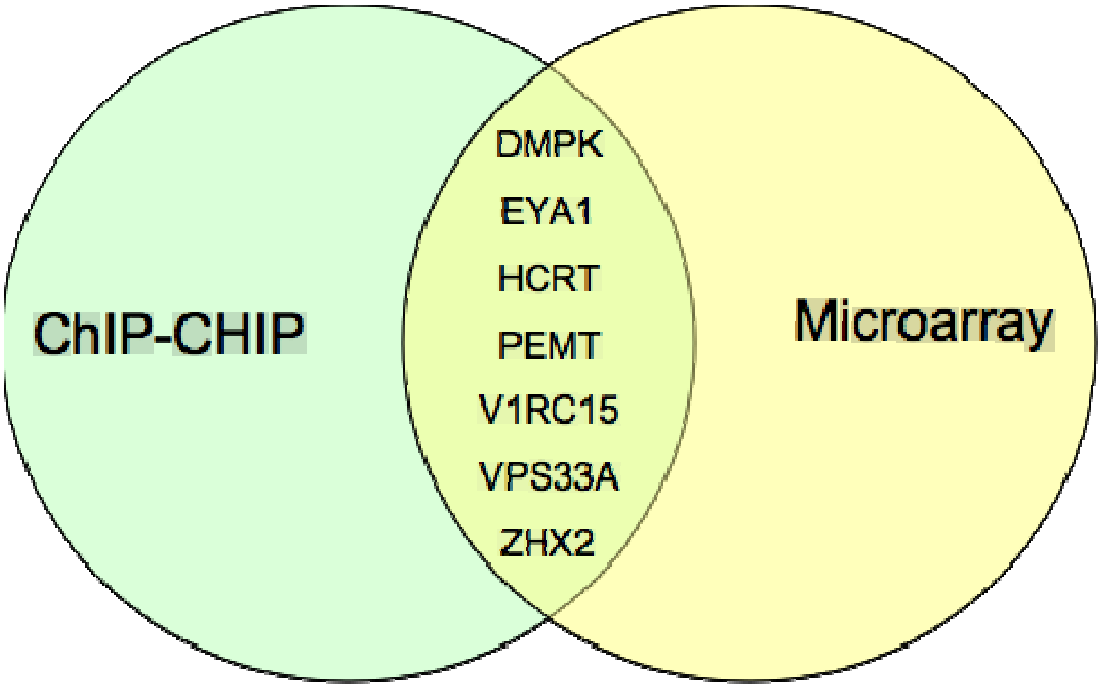
ChIP-CHIP
DMPK
EYA1
HCRT
PEMT
V1RC15
VPS33A
ZHX2
Microarray

Figure S3 Expression profile of human MLIP in patients with Duchenne muscular dystrophy (DMD) Biopsies of normal and diseased quadriceps skeletal muscle tissue of patients with DMD. GDS610 / 54910_at / C6orf142 / Homo sapiens (Haslett JN *et al*, 2003).

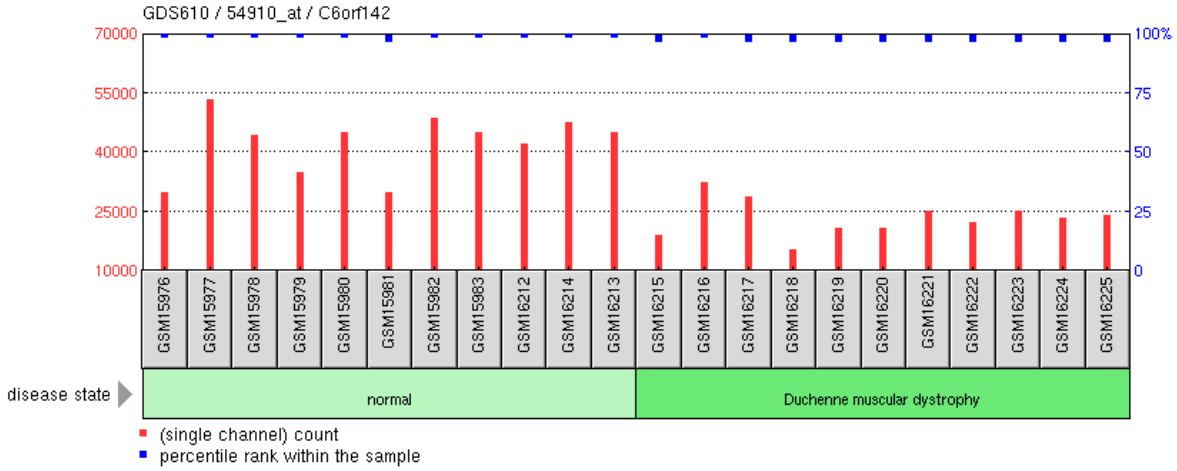
GDS610 / 54910_at / C6orf142
70000
55000
40000
25000
10000
100%
75
50
25
0
GSM15976
GSM15977
GSM15978
GSM15979
GSM15980
GSM15981
GSM15982
GSM15983
GSM16212
GSM16214
GSM16213
GSM16215
GSM16216
GSM16217
GSM16218
GSM16219
GSM16220
GSM16221
GSM16222
GSM16223
GSM16224
GSM16225
disease state
normal
Duchenne muscular dystrophy
(single channel) count
percentile rank within the sample

Figure S4 Expression profile of human MLIP in patients with limb girdle muscular dystrophy 2A (LGMD2A) Biopsies of normal and diseased skeletal muscle tissue of patients with LGMD2A. GDS3475 / 235377_at / C6orf142 / Homo sapiens (Sáenz A *et al*, 2008).

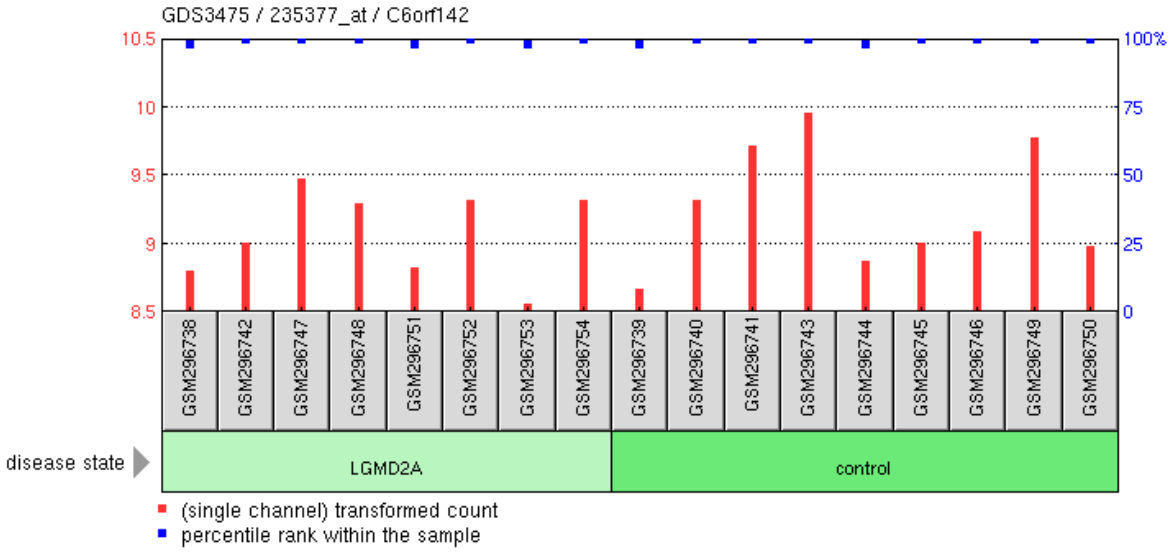
GDS3475 / 235377_at / C6orf142
10.5
10
9.5
9
8.5
100%
75
50
25
0
GSM296738
GSM296742
GSM296747
GSM296748
GSM296751
GSM296752
GSM296753
GSM296754
GSM296739
GSM296740
GSM296741
GSM296743
GSM296744
GSM296745
GSM296746
GSM296749
GSM296750
disease state
LGMD2A
control
(single channel) transformed count
percentile rank within the sample

Figure S5 Expression profile of human MLIP in patients with dilated cardiomyopathy (DCM) Biopsies septal myocardial tissue samples from patients with DCM and non-failing hearts. GDS2206 / RZPDp1096H094D / C6orf142 / Homo sapiens (Barth AS *et al*, 2006).

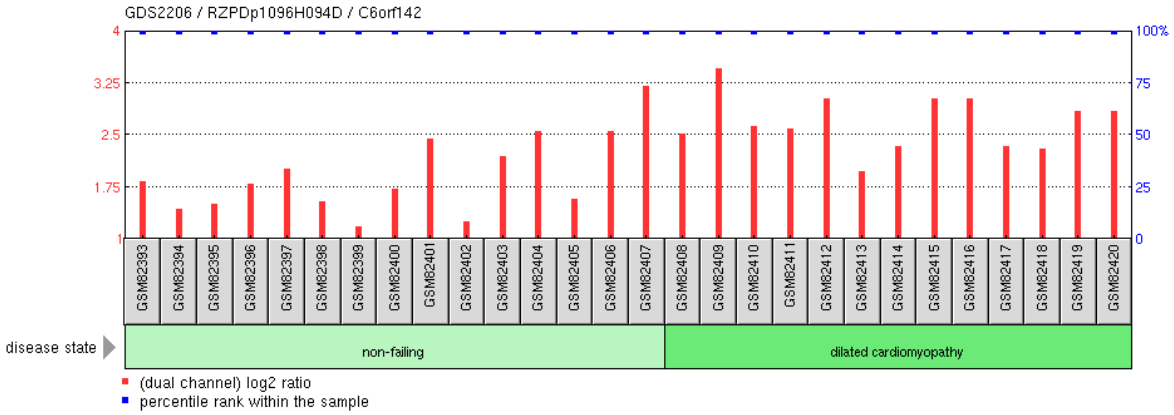
GDS2206 / RZPDp1096H094D / C6orf142
4
3.25
2.5
1.75
1
100%
75
50
25
0
GSM82393
GSM82394
GSM82395
GSM82396
GSM82397
GSM82398
GSM82399
GSM82400
GSM82401
GSM82402
GSM82403
GSM82404
GSM82405
GSM82406
GSM82407
GSM82408
GSM82409
GSM82410
GSM82411
GSM82412
GSM82413
GSM82414
GSM82415
GSM82416
GSM82417
GSM82418
GSM82419
GSM82420
disease state
non-failing
dilated cardiomyopathy
(dual channel) log2 ratio
percentile rank within the sample

Figure S6 Expression profile analysis of MLIP in different tissues of 10 to 12 week old mice Analysis of 22 different tissues from 10 to 12 week old C57BL/6 animals. GDS3142 / 1453059_at / 2310046A06Rik / Mus musculus (Thorrez L et al, 2008).

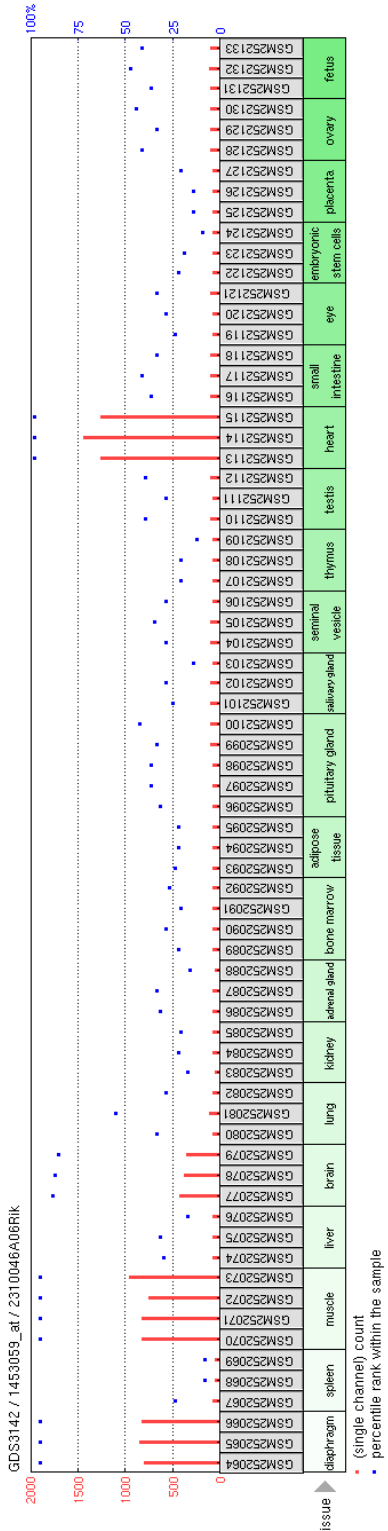
GDS3142 / 1453059_at / 2310046A06Rik
2000
1500
1000
500
0
100%
75
50
25
0
tissue
diaphragm
spleen
muscle
liver
brain
lung
kidney
adrenal gland
bone marrow
adipose tissue
pituitary gland
salivary gland
seminal vesicle
thymus
testis
heart
small intestine
eye
embryonic stem cells
placenta
ovary
fetus
(single channel) count
percentile rank within the sample

Figure S7: Generation of a MLIP conditional knockout (cKO) Mouse Model. A) Targeting vector for MLIP cKO. B) Confirmed targeting and insertion of MLIP targeting vector in mouse ES cells. C) Confirmation of germline transmission of MLIP floxed allele to establish a MLIP conditional KO mouse model.

A)

MLIP cKO Targeting Vector

B)

MLIP Targeted Allele and ES Cell Screening

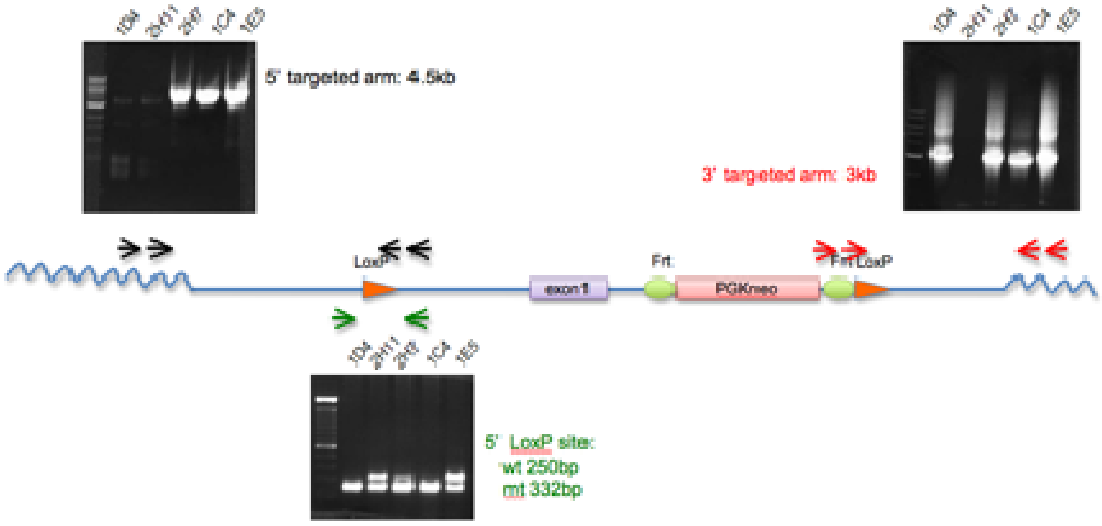

C)

MLIP targeting Confirmation

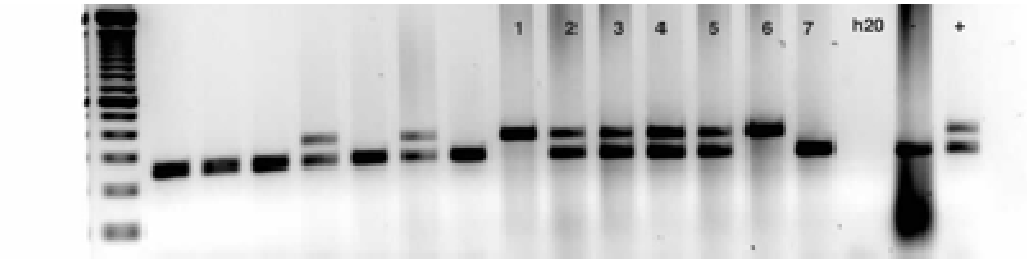

Table S3. Genotype distribution from 5 $MLIP^{+/fl}$; CMV-Cre x $MLIP^{fl/fl}$ crosses

Genotype	Expected Fraction	Actual Number born
$MLIP^{+/fl}$	0.25	9
$MLIP^{fl/fl}$	0.25	13
$MLIP^{+/fl}$; CMV-cre	0.25	11
$MLIP^{fl/fl}$; CMV-cre	0.25	0

Chi squared equals 11.970 with 3 degrees of freedom (p = 0.0075)

Table S4. Heart to Body weight of heterozygous MLIP mouse model. (females 10 weeks of age)

Genotype	Body Weight (g)	Heart Weight (mg)	Heart:Body Weight
$MLIP^{fl/fl}$	18.1±1.53	115±9.54	6.35±0.25
Cre-CMV; $MLIP^{+/-}$	17.8±2.57	108±15	6.08±0.15
*P**	NS	NS	0.172

*T-test $MLIP^{fl/fl}$ vs CMV-cre $MLIP^{+/-}$, n=3

Figure S8: MLIP protein expression in heart and skeletal muscle tissue in MLIP heterozygous mice Hearts and skeletal muscle were collected from two adult female wild type mice and two adult female MLIP +/- mice. Tissues were lysed for Western blot detection, probing for MLIP and lamin A/C expression. GAPDH was used as the loading control.

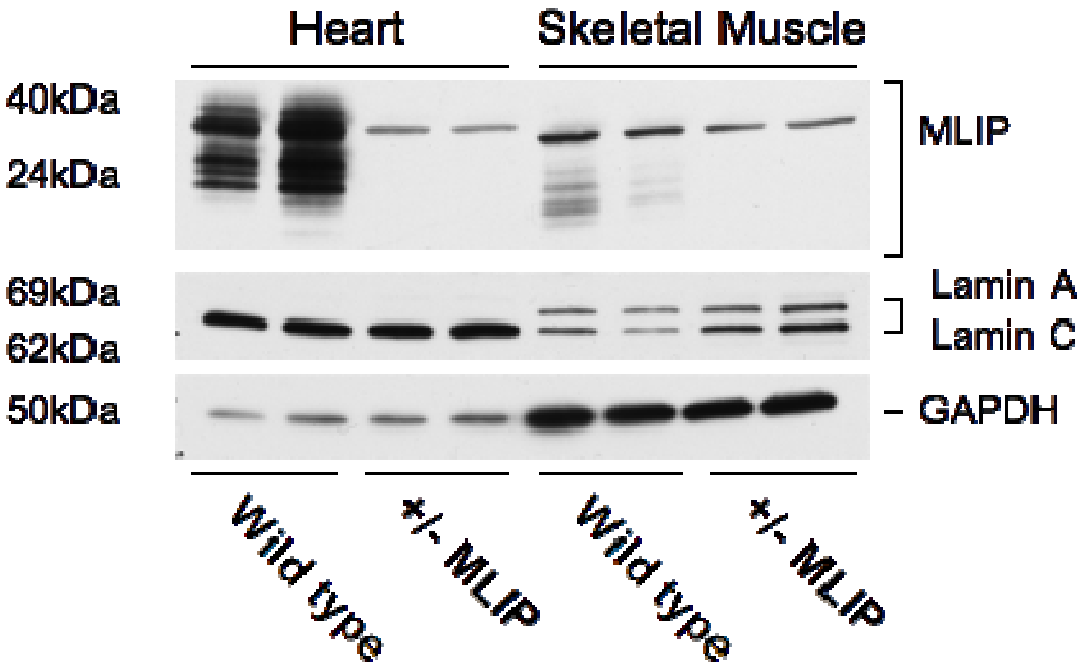
Heart
Skeletal Muscle
40kDa
24kDa
MLIP
69kDa
62kDa
Lamin A
Lamin C
50kDa
GAPDH
Wild type
+/- MLIP
Wild type
+/- MLIP

References

Abdelhak, S., Kalatzis, V., Heilig, R., Compain, S., Samson, D., Vincent, C., Levi-Acobas, F., Cruaud, C., Le Merrer, M., Mathieu, M.*, et al.* (1997). Clustering of mutations responsible for branchio-oto-renal (BOR) syndrome in the eyes absent homologous region (eyaHR) of EYA1. Hum. Mol. Genet. *6,* 2247-2255.

Andres, V., and Gonzalez, J.M. (2009). Role of A-type lamins in signaling, transcription, and chromatin organization. J. Cell Biol. *187,* 945-957.

Barth, A.S., Kuner, R., Buness, A., Ruschhaupt, M., Merk, S., Zwermann, L., Kääb, S., Kreuzer, E., Steinbeck, G., Mansmann, U.*, et al.* (2006). Identification of a Common Gene Expression Signature in Dilated Cardiomyopathy Across Independent Microarray Studies. J. Am. Coll. Cardiol. *48,* 1610-1617.

Beck, L.A., Hosick, T.J., and Sinensky, M. (1990). Isoprenylation is required for the processing of the lamin A precursor. J. Cell Biol. *110,* 1489-1499.

Berger, P., Young, P., and Suter, U. (2002). Molecular cell biology of Charcot-Marie-Tooth disease. Neurogenetics *4,* 1-15.

Biamonti, G., Giacca, M., Perini, G., Contreas, G., Zentilin, L., Weighardt, F., Guerra, M., Della Valle, G., Saccone, S., and Riva, S. (1992). The gene for a novel human lamin maps at a highly transcribed locus of chromosome 19 which replicates at the onset of S-phase. Mol. Cell. Biol. *12,* 3499-3506.

Bione, S., Maestrini, E., Rivella, S., Mancini, M., Regis, S., Romeo, G., and Toniolo, D. (1994). Identification of a novel X-linked gene responsible for Emery-Dreifuss muscular dystrophy. Nat. Genet. *8,* 323-327.

Boucher, C.A., King, S.K., Carey, N., Krahe, R., Winchester, C.L., Rahman, S., Creavin, T., Meghji, P., Bailey, M.E.S., Chartier, F.L.*, et al.* (1995). A novel homeodomain-encoding gene is associated with a large CpG island interrupted by the myotonic dystrophy unstable (CTG)n repeat. Hum. Mol. Genet. *4,* 1919-1925.

Burke, B., Mounkes, L.C., and Stewart, C.L. (2001). The nuclear envelope in muscular dystrophy and cardiovascular diseases. Traffic *2,* 675-683.

Capell, B.C., and Collins, F.S. (2006). Human laminopathies: nuclei gone genetically awry. Nat. Rev. Genet. *7,* 940-952.

Chen, I.-.B., Huber, M., Guan, T., Bubeck, A., and Gerace, L. (2006). Nuclear envelope transmembrane proteins (NETs) that are up-regulated during myogenesis. BMC Cell Biol. *7,*

D'Angelo, M.A., and Hetzer, M.W. (2006). The role of the nuclear envelope in cellular organization. Cell Mol. Life Sci. *63,* 316-332.

De Jonghe, P., Mersivanova, I., Nelis, E., Favero, J.D., Martin, J.-., Van Broeckhoven, C., Evgrafov, O., and Timmerman, V. (2001). Further evidence that neurofilament light chain gene mutations can cause Charcot-Marie-Tooth disease type 2E. Ann. Neurol. *49,* 245-249.

De la Luna, S., and Ortin, J. (1992). [33] pac Gene as efficient dominant marker and reporter gene in mammalian cells. METHODS ENZYMOL. *216,* 376-385.

Di Padova, M., Caretti, G., Zhao, P., Hoffman, E.P., and Sartorelli, V. (2007). MyoD acetylation influences temporal patterns of skeletal muscle gene expression. J. Biol. Chem. *282,* 37650-37659.

Fatkin, D., McConnell, B.K., Mudd, J.O., Semsarian, C., Moskowitz, I.G.P., Schoen, F.J., Giewat, M., Seidman, C.E., and Seidman, J.G. (2000). An abnormal Ca2+ response in mutant sarcomere protein-mediated familial hypertrophic cardiomyopathy. J. Clin. Invest. *106,* 1351-1359.

Fougerousse, F., Durand, M., Lopez, S., Suel, L., Demignon, J., Thornton, C., Ozaki, H., Kawakami, K., Barbet, P., Beckmann, J.S., and Maire, P. (2002). Six and Eya expression during human somitogenesis and MyoD gene family activation. J. Muscle Res. Cell. Motil. *23,* 255-264.

Gerace, L., and Blobel, G. (1980). The nuclear envelope lamina is reversibly depolymerized during mitosis. Cell *19,* 277-287.

Goldman, R.D., Shumaker, D.K., Erdos, M.R., Eriksson, M., Goldman, A.E., Gordon, L.B., Gruenbaum, Y., Khuon, S., Mendez, M., Varga, R., and Collins, F.S. (2004). Accumulation of mutant lamin A causes progressive changes in nuclear architecture in Hutchinson-Gilford progeria syndrome. Proc. Natl. Acad. Sci. U. S. A. *101,* 8963-8968.

Gruenbaum, Y., Margalit, A., Goldman, R.D., Shumaker, D.K., and Wilson, K.L. (2005). The nuclear lamina comes of age. Nat. Rev. Mol. Cell Biol. *6,* 21-31.

Harmon, E.B., Harmon, M.L., Larsen, T.D., Paulson, A.F., and Perryman, M.B. (2008). Myotonic dystrophy protein kinase is expressed in embryonic myocytes and is required for myotube formation. Dev. Dyn. *237,* 2353-2366.

Haslett, J.N., Sanoudou, D., Kho, A.T., Han, M., Bennett, R.R., Kohane, I.S., Beggs, A.H., and Kunkel, L.M. (2003). Gene expression profiling of Duchenne muscular dystrophy skeletal muscle. Neurogenetics *4,* 163-171.

Hegele, R.A., Cao, H., Liu, D.M., Costain, G.A., Charlton-Menys, V., Rodger, N.W., and Durrington, P.N. (2006). Sequencing of the reannotated LMNB2 gene reveals novel mutations in patients with acquired partial lipodystrophy. Am. J. Hum. Genet. *79,* 383-389.

Heitlinger, E., Peter, M., Lustig, A., Villiger, W., Nigg, E.A., and Aebi, U. (1992). The role of the head and tail domain in lamin structure and assembly: analysis of bacterially expressed chicken lamin A and truncated B2 lamins. J. Struct. Biol. *108,* 74-89.

Holaska, J.M. (2008). Emerin and the nuclear lamina in muscle and cardiac disease. Circ. Res. *103,* 16-23.

Huang, D.W., Sherman, B.T., and Lempicki, R.A. (2009). Bioinformatics enrichment tools: Paths toward the comprehensive functional analysis of large gene lists. Nucleic Acids Res. *37,* 1-13.

Huang, D.W., Sherman, B.T., and Lempicki, R.A. (2009). Systematic and integrative analysis of large gene lists using DAVID bioinformatics resources. Nat. Protoc. *4,* 44-57.

Hutchison, C.J. (2002). Lamins: building blocks or regulators of gene expression? Nat. Rev. Mol. Cell Biol. *3,* 848-858.

Irobi, J., De Jonghe, P., and Timmerman, V. (2004). Molecular genetics of distal hereditary motor neuropathies. Hum. Mol. Genet. *13,* R195-R202.

Ismailov, S.M., Fedotov, V.P., Dadali, E.L., Polyakov, A.V., Van Broeckhoven, C., Ivanov, V.I., De Jonghe, P., Timmerman, V., and Evgrafov, O.V. (2001). A new locus for autosomal dominant Charcot-Marie-Tooth disease type 2 (CMT2F) maps to chromosome 7q11-q21. Eur. J. Hum. Genet. *9,* 646-650.

Johnson, K.J., Boucher, C.A., King, S.K., Winchester, C.L., Bailey, M.E.S., Hamilton, G.M., and Carey, N. (1996). Is myotonic dystrophy a single-gene disorder? Biochem. Soc. Trans. *24,* 510-513.

Klesert, T.R., Cho, D.H., Clark, J.I., Maylie, J., Adelman, J., Snider, L., Yuen, E.C., Soriano, P., and Tapscott, S.J. (2000). Mice deficient in Six5 develop cataracts: Implications for myotonic dystrophy. Nat. Genet. *25,* 105-109.

Klesert, T.R., Otten, A.D., Bird, T.D., and Tapscott, S.J. (1997). Trinucleotide repeat expansion at the myotonic dystrophy locus reduces expression of DMAHP. Nat. Genet. *16,* 402-406.

Koh, W., Jeong, S.-., Lee, H.-., Ryu, H.-., Lee, E.-., Ahn, K.S., Bae, H., and Kim, S.-. Melatonin promotes puromycin-induced apoptosis with activation of caspase-3 and 5'-adenosine monophosphate-activated kinase-alpha in human leukemia HL-60 cells. J. Pineal Res.

Krimm, I., Ostlund, C., Gilquin, B., Couprie, J., Hossenlopp, P., Mornon, J.P., Bonne, G., Courvalin, J.C., Worman, H.J., and Zinn-Justin, S. (2002). The Ig-like structure of the C-terminal domain of lamin A/C, mutated in muscular dystrophies, cardiomyopathy, and partial lipodystrophy. Structure *10,* 811-823.

Kuang, S., Gillespie, M.A., and Rudnicki, M.A. (2008). Niche regulation of muscle satellite cell self-renewal and differentiation. Cell. Stem Cell. *2,* 22-31.

Lallemand-Breitenbach, V., and de The, H. (2010). PML nuclear bodies. Cold Spring Harb Perspect. Biol. *2,* a000661.

Lin, F., and Worman, H.J. (1993). Structural organization of the human gene encoding nuclear lamin A and nuclear lamin C. J. Biol. Chem. *268,* 16321-16326.

Martin, C., Chen, S., Maya-Mendoza, A., Lovric, J., Sims, P.F., and Jackson, D.A. (2009). Lamin B1 maintains the functional plasticity of nucleoli. J. Cell. Sci. *122,* 1551-1562.

Maske, C.P., Hollinshead, M.S., Higbee, N.C., Bergo, M.O., Young, S.G., and Vaux, D.J. (2003). A carboxyl-terminal interaction of lamin B1 is dependent on the CAAX endoprotease Rce1 and carboxymethylation. J. Cell Biol. *162,* 1223-1232.

Merlini L. Neuromuscular Disorders (January 2001), 11(1), 102. (http://umd.be//LMNA/)

Moran, D.M., Shen, H., and Maki, C.G. (2009). Puromycin-based vectors promote a ROS-dependent recruitment of PML to nuclear inclusions enriched with HSP70 and proteasomes. BMC Cell Biol. *10,*

Muchir, A., Pavlidis, P., Decostre, V., Herron, A.J., Arimura, T., Bonne, G., and Worman, H.J. (2007). Activation of MAPK pathways links LMNA mutations to cardiomyopathy in Emery-Dreifuss muscular dystrophy. J. Clin. Invest. *117,* 1282-1293.

Nigg, E.A. (1992). Assembly and cell cycle dynamics of the nuclear lamina. Semin. Cell Biol. *3,* 245-253.

Olguin, H.C., and Olwin, B.B. (2004). Pax-7 up-regulation inhibits myogenesis and cell cycle progression in satellite cells: a potential mechanism for self-renewal. Dev. Biol. *275,* 375-388.

Padiath, Q.S., Saigoh, K., Schiffmann, R., Asahara, H., Yamada, T., Koeppen, A., Hogan, K., Ptacek, L.J., and Fu, Y.H. (2006). Lamin B1 duplications cause autosomal dominant leukodystrophy. Nat. Genet. *38,* 1114-1123.

Parker, M.H., Seale, P., and Rudnicki, M.A. (2003). Looking back to the embryo: defining transcriptional networks in adult myogenesis. Nat. Rev. Genet. *4,* 497-507.

Perdiguero, E., Sousa-Victor, P., Ballestar, E., and Munoz-Canoves, P. (2009). Epigenetic regulation of myogenesis. Epigenetics *4,* 541-550.

Reddel, C.J., and Weiss, A.S. (2004). Lamin A expression levels are unperturbed at the normal and mutant alleles but display partial splice site selection in Hutchinson-Gilford progeria syndrome. J. Med. Genet. *41,* 715-717.

Rober, R.A., Weber, K., and Osborn, M. (1989). Differential timing of nuclear lamin A/C expression in the various organs of the mouse embryo and the young animal: a developmental study. Development *105,* 365-378.

Sabourin, L.A., and Rudnicki, M.A. (2000). The molecular regulation of myogenesis. Clin. Genet. *57,* 16-25.

Sáenz, A., Azpitarte, M., Armañanzas, R., Leturcq, F., Alzualde, A., Inza, I., García-Bragado, F., De la Herran, G., Corcuera, J., Cabello, A.*, et al.* (2008). Gene expression profiling in limb-girdle muscular dystrophy 2A. PLoS ONE *3,*

Sarkar, P.S., Appukuttan, B., Han, J., Ito, Y., Ai, C., Tsai, W., Chai, Y., Stout, J.T., and Reddy, S. (2000). Heterozygous loss of Six5 in mice is sufficient to cause ocular cataracts. Nat. Genet. *25,* 110-114.

Shackleton, S., Lloyd, D.J., Jackson, S.N., Evans, R., Niermeijer, M.F., Singh, B.M., Schmidt, H., Brabant, G., Kumar, S., Durrington, P.N.*, et al.* (2000). LMNA, encoding lamin A/C, is mutated in partial lipodystrophy. Nat. Genet. *24,* 153-156.

Spitz, F., Demignon, J., Porteu, A., Kahn, A., Concordet, J.-., Daegelen, D., and Maire, P. (1998). Expression of myogenin during embryogenesis is controlled by six/sine oculis homeoproteins through a conserved MEF3 binding site. Proc. Natl. Acad. Sci. U. S. A. *95,* 14220-14225.

Stuurman, N., Heins, S., and Aebi, U. (1998). Nuclear lamins: their structure, assembly, and interactions. J. Struct. Biol. *122,* 42-66.

Stuurman, N., Meijne, A.M., van der Pol, A.J., de Jong, L., van Driel, R., and van Renswoude, J. (1990). The nuclear matrix from cells of different origin. Evidence for a common set of matrix proteins. J. Biol. Chem. *265,* 5460-5465.

Susa, T., Kato, T., and Kato, Y. (2008). Reproducible transfection in the presence of carrier DNA using FuGENE6 and Lipofectamine 2000. Mol. Biol. Rep. *35,* 313-319.

Tang, B.-., Zhao, G.-., Luo, W., Xia, K., Cai, F., Pan, Q., Zhang, R.-., Zhang, F.-., Liu, X.-., Chen, B.*, et al.* (2005). Small heat-shock protein 22 mutated in autosomal dominant Charcot-Marie-Tooth disease type 2L. Hum. Genet. *116,* 222-224.

Thorrez, L., Van Deun, K., Tranchevent, L.-., Van Lommel, L., Engelen, K., Marchal, K., Moreau, Y., Van Mechelen, I., and Schuit, F. (2008). Using ribosomal protein genes as reference: A tale of caution. PLoS ONE *3,*

Untergasser A. “RNAprep - TRIzol combined with Columns” *Untergasser's Lab*. Winter 2008.(02-Novermber-2009).
<http://www.untergasser.de/lab/protocols/rna_prep_comb_TRIzol_v1_0.htm>.

Vázquez, D. (1979). Inhibitors of protein biosynthesis. Mol. Biol. Biochem. Biophys. *30,* i-x, 1-312.

Vergnes, L., Peterfy, M., Bergo, M.O., Young, S.G., and Reue, K. (2004). Lamin B1 is required for mouse development and nuclear integrity. Proc. Natl. Acad. Sci. U. S. A. *101,* 10428-10433.

Wang, Z.-., Ruggero, D., Ronchetti, S., Zhong, S., Gaboli, M., Rivi, R., and Pandolfi, P.P. (1998). Pml is essential for multiple apoptotic pathways. Nat. Genet. *20,* 266-272.

Winchester, C.L., Ferrier, R.K., Sermoni, A., Clark, B.J., and Johnson, K.J. (1999). Characterization of the expression of DMPK and SIX5 in the human eye and implications for pathogenesis in myotonic dystrophy. Hum. Mol. Genet. *8,* 481-492.

Worman, H.J., Fong, L.G., Muchir, A., and Young, S.G. (2009). Laminopathies and the long strange trip from basic cell biology to therapy. J. Clin. Invest. *119,* 1825-1836.

Worman, H.J., Ostlund, C., and Wang, Y. (2010). Diseases of the nuclear envelope. Cold Spring Harb Perspect. Biol. *2,* a000760.

Wrześniok, D., Surazyński, A., Karna, E., Buszman, E., and Pałka, J. (2005). Melanin counter act puromycin-induced inhibition of collagen and DNA biosynthesis in human skin fibroblasts. Life Sci. *77,* 528-538.

Yamano, S., Dai, J., and Moursi, A.M. (2010). Comparison of transfection efficiency of nonviral gene transfer reagents. Mol. Biotechnol. *46,* 287-300.

Zammit, P.S., Golding, J.P., Nagata, Y., Hudon, V., Partridge, T.A., and Beauchamp, J.R. (2004). Muscle satellite cells adopt divergent fates: a mechanism for self-renewal? J. Cell Biol. *166,* 347-357.

Zhang, F.L., and Casey, P.J. (1996). Protein prenylation: molecular mechanisms and functional consequences. Annu. Rev. Biochem. *65,* 241-269.

Zhong, S., Salomoni, P., and Pandolfi, P.P. (2000). The transcription role of PML and the nuclear body. Nature Cell Biol. *2,* E85-E90.